ISSN 0024-4902, Lithology and Mineral Resources, 2016, Vol. 51, No. 4, pp. 310–332. © Pleiades Publishing, Inc., 2016.
Original Russian Text © A.I. Khisamutdinova, A.V. Solov'ev, D.V. Rozhkova, 2016, published in Litologiya i Poleznye Iskopaemye, 2016, No. 4, pp. 359–383.

Provenance Analysis for Middle Eocene Sediments in the West Kamchatka Sedimentary Basin (Tigil Area)

A. I. Khisamutdinova[a], A. V. Solov'ev[a, b], and D. V. Rozhkova[c]

[a]*Geological Institute, Russian Academy of Sciences (GIN), Pyzhevskii per. 7, Moscow, 119017 Russia*
e-mail: geoaisulu@gmail.com
[b]*Dal'morneftegeozika Open Joint Stock Company (DMNG), pr. Mira 426, Yuzhno-Sakhalinsk, 693004 Russia*
e-mail: fission-track@mail.ru
[c]*Polimetall JSC , ul. Flegontova 24, Khabarovsk, 680000 Russia*
e-mail: duvir19@gmail.com

Received April 6, 2015

Abstract—The paper presents the results of reconstruction of Middle Eocene provenances for the West Kamchatka sedimentary basin (WKSB) corresponding to the Tigil area. It has been established that the early (Eocene) evolution stage of WKSB was marked by the deposition of terrigenous sediments in intermontane depressions followed by the accumulation of shallow-marine sediments after transgression. In terms of the composition, sandstones of the Middle Eocene Snatol Formation correspond to graywackes. With respect to the geochemistry of sandstones, their provenances were confined to an active continental margin and island arc. The mineral composition of the heavy fraction suggests an alternating dominance of felsic and mafic rocks in the provenances. Dating of the clastic zircon from sandstones of the Snatol Formation by the LA-ICP-MS method revealed a wide variation range of their age. The most significant peak is close to the age of calc-alkaline magmatism in the Okhotsk–Chukotka volcanic belt. This fact provides insight into the Eocene paleogeography: the major rock provenances were located in the Okhotsk–Chukotka volcanic belt and the eastern Achaivayam–Valagin island arc. Local sources of clastic material were represented by the Utkholok and Kinkil volcanic belts.

DOI: 10.1134/S0024490216040039

Reconstruction of the Cenozoic evolution of WKSB is important for deciphering geodynamic processes in the Sea of Okhotsk region and estimating petroleum potential of this structure. The early (Paleocene–Eocene) stage of WKSB, i.e., origination and evolution of the West Kamchatka trough is least studied. The stratigraphic subdivision of the Paleocene–Eocene sequence, its dislocation pattern, and paleogeographic reconstructions of this stage are debatable (Belonin et al., 2003; Bogdanov and Chekhovich, 2002; Gladenkov et al., 1997; Moiseev and Solov'ev, 2010). It should be noted that the lower WKSB section is promising for the detection of hydrocarbons, because Late Paleocene(?)–Eocene terrigenous rocks are potential reservoirs (Belonin et al., 2003; *Otchet* ..., 1986).

Our studies were aimed at reconstruction of the source of clastic material transported to WKSB in the Middle Eocene. The paper presents data on the mineral and chemical compositions and the heavy fraction of sandstones of the Middle Eocene Snatol Formation. We also examined the U–Pb age and crystal morphology of clastic zircon from these sandstones. The comprehensive analysis of these data made it possible to reconstruct possible provenances of the clastic material and propose new paleogeographic models.

GEOLOGICAL AND TECTONIC SETTING OF THE TAGIL UPLIFT

The northeastern part of Asia is a collage of different-age heterogeneous terranes incorporated into Eurasia in the Mesozoic and Cenozoic (Bogdanov and Chekhovich, 2002; Bogdanov and Dobretsov, 2002; Nokleberg et al., 1998; *Ob'yasnitel'naya zapiska* ..., 2000; Parfenov et al., 1993; Sokolov, 1992; Stavsky et al., 1990; Til'man et al., 1992; Watson and Fujita, 1985; Worrall, 1991; Zinkevich et al., 1993; Zonnenshain et al., 1990).

The basement of western Kamchatka is considered a part of the Sea of Okhotsk Plate in (Gladenkov et al., 1997; Khanchuk, 1985; Konstantinovskaia, 2001), but it is defined as an independent West Kamchatka microplate in (Bogdanov and Chekhovich, 2002; *Ob"yasnitel'naya zapiska* ..., 2000). The Sea of Okhotsk Plate is considered the fragment of an ancient oceanic plateau (Bogdanov and Dobretsov, 2002), whereas the West Kamchatka microplate is located in the continental-type crust (Bogdanov and Chekhovich, 2002).

The basement of WKSB is composed of terrigenous rocks of the Omgon–Ukelayat terrane and silicic volcanic rocks of the Achaivayam–Valagin island arc.

The Omgon–Ukelayat terrane comprises Late Cretaceous–Middle Eocene terrigenous rocks that are exposed in northern Kamchatka Peninsula and Omgon Range. According to (Solov'ev and Shapiro, 2008), terrigenous sediments of the Omgon–Ukelayat terrane are turbidites and contourites that were deposited in the Cretaceous–Middle Eocene along the northeastern margin of Asia.

The Achaivayam–Valagin island arc includes Late Cretaceous siliceous and volcanic rocks that are exposed in erosional "windows" in the central and eastern parts of western Kamchatka. According to (Solov'ev et al., 2011), the island arc was incorporated into the margin of Asia in the Eocene that marked the onset of the WKSB formation.

The Tigil uplift, which includes the studied sections, is located in the central WKSB. The NE-striking uplift is about 300 km long and 100–120 km wide. The uplift comprises the Uvuchin anticline and the conjugated Mainach low-angle syncline. According to (*Skhema* ..., 2001), the northern Tochilin anticline is confined to the Kinkil trough. The uplift comprises brachioform and linear folds with limbs dipping at 30°–40°. The Cenozoic sequence is crosscut by faults parallel and perpendicular to the structural fabric. The central part of the uplift is composed of Cretaceous and Lower Paleogene rocks.

STRATIGRAPHY

The Paleogene basement in the Tigil uplift includes three formations (from the bottom to top): Khulgun (conglomerate), Napan (coaliferous), and Snatol (mainly, sandy) (*Karta* ..., 1999; *Resheniya* ..., 1998). Beginning from the Snatol Formation and stratigraphically upward (Pliocene included), the Tigil uplift is marked by a consistent succession of Cenozoic sediments, with stratotype sections exposed along the Sea of Okhotsk coast.

The lower WKSB section is a continental sequence marked by small thickness and conglomerate lenses deposited in intermontane depressions and foothills (Grigorenko, 2011). The conglomerates unconformably overlie protrusions of the Cretaceous basement and make up the basal part of coastal sections (Mainach and Uvuchin), as well as ledges along the bank of large Kvachina and Snatolveem rivers (Fig. 1). Based on flora finds, the age of conglomerates is estimated as Paleocene (Budantsev, 2006; Gladenkov et al., 1997). According to our data (Khisamutdinova et al., 2015), conglomerates exposed in coastal sections are younger. Based on the K–Ar dating of amphibole and biotite from conglomerate pebbles, the lower limit of the coarse-clastic sequence deposition corresponds to the Eocene.

Conglomerates of the Khulgun Formation are irregularly overlain by the coaliferous sandstones intercalating with conglomerates of the Napan Formation. Its stratotype is recorded in the Snatolveem River valley (Gladenkov et al., 1997). The Napan Formation in this section makes up the core of a steep anticline. The outcrop is crosscut by overthrusts, along which rocks of the Napan Formation are discordantly overlain by Middle Eocene sandstones of the Snatol Formation. The coaliferous sandstones were deposited in the continental setting within a hilly plain with periodically flooded sectors (Grigorenko, 2011). The Napan Formation includes foraminifers, rare macrofauna, and leafy flora. Based on their finds, age of the Napan Formation is estimated as Late Paleocene–Early Eocene (Budantsev, 2006; Gladenkov et al., 1997).

We studied the Snatol Formation mainly composed of sandstones with rare interbeds of conglomerates and clayey rocks. These rocks lie unconformably (conformably in some places) over the basal conglomerates assigned in various sections to the Khulgun Formation (Paleocene) or Snatol Formation (Middle Eocene) that overlie the Cretaceous basement. In some sections, sandstones of the Snatol Formation lie with angular and stratigraphic unconformity over the Cretaceous basement (Solov'ev, 2005). Tectonic contact between the Napan and Snatol formations is defined on the right bank of the Snatolveem River (Gladenkov et al., 1997). The base of the Napan Formation is unexposed.

The Snatol Formation is widespread over the entire WKSB. According to (*Resheniya* ..., 1998), the Rategin and Ust-Anadyr formations are developed in the coeval sections of the Chemurnaut Bay and Palan area in the northern part of the basin. Thickness of Middle Eocene sediments varies from the north (300–400 m) to south (50–100 m) and reaches the maximum in the Tigil uplift (500–1000 m) (*Resheniya* ..., 1998). This formation pinches out in the southern part of WKSB.

The detailed paleontological characteristics of the lower part of this sedimentary section are given in (Dmitrieva, 2007; Gladenkov et al., 1991, 1997, 2005; Serova, 2001). The faunal assemblage is mainly represented by marine mollusks and benthic foraminifers that often contain the endemic species.

It is noteworthy that the sequential bedding of Paleocene–Eocene formations is lacking in any lower WKSB sections or in available publications.

HISTORY OF THE STUDY OF WKSB

A significant contribution to the study of lithology and stratigraphic subdivision of the lower WKSB section was made by workers from GIN (Gladenkov et al., 1991, 1997, 2005) and VNIGRI (All-Russia Geological Prospecting Research Institute). Assessment of the hydrocarbon potential of sedimentary structures and intervals were carried out by researchers from MGU (Moscow State University) and VNIGRI (Belonin et al., 2003; Grigorenko et al., 1969, 1981, 2011; Svistunov et al., 1977).

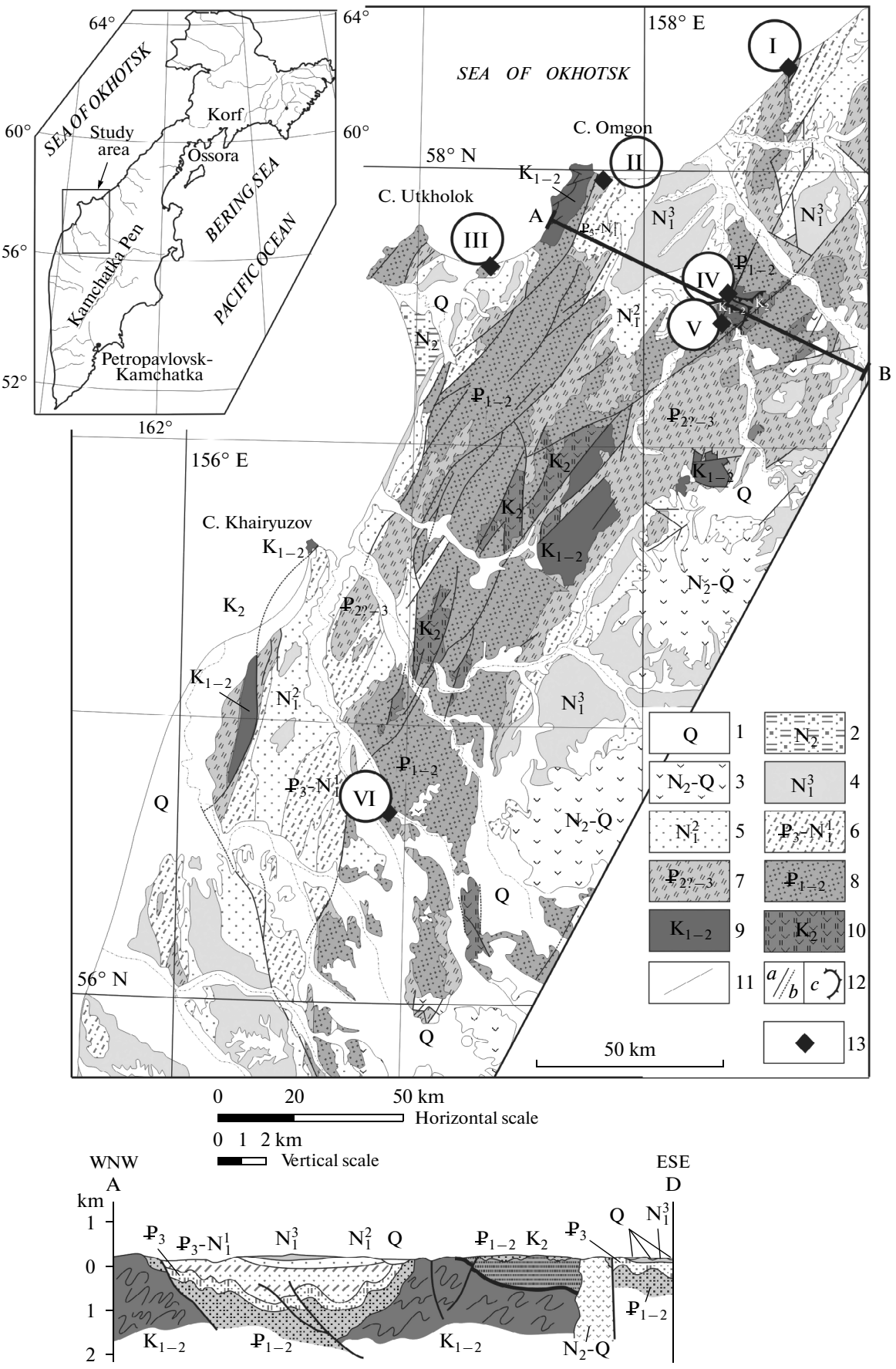
64°
60°
56°
52°
SEA OF OKHOTSK
Korf
Study area
Ossora
BERING SEA
PACIFIC OCEAN
Kamchatka Pen
Petropavlovsk-Kamchatka
162°
156° E
158° E
58° N
56° N
SEA OF OKHOTSK
C. Omgon
C. Utkholok
C. Khairyuzov
I
II
III
IV
V
VI
A
B
Q
N2
N2-Q
N13
N23
P1–2
P2?–3
P3-N11
K1–2
K2
50 km
0 20 50 km
Horizontal scale
0 1 2 km
Vertical scale
WNW
ESE
A
D
km
1
0
1
2

Fig. 1. Schematic geological setting of the central part of western Kamchatka. Modified after (*Karta* ..., 1999; Gladenkov et al., 1997). (1–8) Sediments of the West Kamchatka trough: (1) Quaternary, (2) N_2 (Enemten Formation), (3) N_2–Q, volcanic, (4) N_1^3 (hereinafter, from the bottom to top): Etolon and Ermanov formations), (5) N_1^2 (ll'in and Kakert formations), (6) (P_3-N_1^1 (Viventek and Kuluven formations), (7) P_3 (Amanin, Gakkhin, and Utkholok formations), (8) P_{1-2} (Khulgun, Napan, and Snatol formations plus Kovachin Group); (9, 10) trough basement: (9) K_{1-2}, flyschoid sediments of autochthon (Tal'nich, Mainach, and Kunun formations), (10) K_2, silicic volcanic sediments of allochthon (Irunei Formation); (11) stratigraphic contacts; (12) faults: (*a*) proven, (*b*) inferred, (*c*) overthrust; (13) positions of the studied sections: (I–III) marine coastal sections: (I) Tochilin, (II) Mainach, (III) Uvuchin; (IV–VI) river bank sections: (IV) Rassoshina River, (V) Polovinka River, (VI) Belogolovaya River.

The Paleocene–Early Eocene paleogeographic models based on the lithostratigraphic data without the consideration of palinspastic reconstructions are given in (Gladenkov et al., 1997). These models show the transport of clastic material and possible areas of volcanism within WKSB.

Paleogeographic reconstructions for the later (Late Eocene and Oligocene) interval based on the lithofacies and formational analysis of the Cenozoic section in outcrops and borehole cores are presented in (Belonin et al., 2003). The models show the distribution of lithofacies and various sedimentation settings, but the possible direction of clastic material transport is not indicated.

Scrutinization of the composition and formational affiliation of terrigenous rocks in the lower WKSB section is reported in (Grigorenko, 1969, 1981, 2011). In (Grigorenko, 1981), all sandstones are assigned to the graywacke group, the composition of basal conglomerates is estimated, and the main directions of the clastic material transport from the west and east into the incipient submeridional trough are reconstructed.

METHODS

We carried out a comprehensive study of sandstones based on the standard petrographic and geochemical methods, analysis of the heavy fraction, and detailed study of the detrital zircon (analysis of crystal morphology and U–Pb LA-ICP-MS dating).

Sandstones were examined under a polarization microscope. The composition of major minerals, grain interrelation, and cement type and composition were studied at a magnification of 10. The number of major minerals and rock clasts was calculated at a magnification of 20 (the minimum number of analyzed samples was 300). The number of grains was estimated using the method developed by F. Chase (1963) and modified by M.N. Shapiro. The sandstone composition is summarized in Table 1.

The content of the major components of sandstones was determined by the silicate analysis in the Chemical-Analytical Laboratory of GIN (M.V. Rudchenko, analyst).

The heavy fraction of sandstones was analyzed in the Mineralogical–Track Analysis Laboratory of GIN based on the standard procedure (Kopchenova, 1979): crushing → sieving → panning → magnetic separation → fractionation in the heavy liquid (bromoform) and electromagnetic separation → study of the fraction under binocular microscope. Then, we examined morphology of zircon crystals in the –0.07 mm monofraction by the method described in (Pupin, 1980). The obtained data were compared with the diagram proposed in (Belousova et al., 2006). In our table, the initial table of zircon morphological types (hereafter, morphotypes) according to (Pupin, 1980) is supplemented with information pertaining to the genetic granitoid types characterized by specific crystal habitus.

The age of clastic zircon was determined by the LA-ICP-MS method according to (Gehrels, 2011; Gehrels et al., 2008) at University of Arizona (Tyson, United States).

THE STUDIED SECTIONS

Field studies were carried out in 2005–2008 by the Prospecting Team of GIN in the Tigil uplift area of western Kamchatka. We described and scrutinized sediments of the Snatol Formation in stratotype coastal sections (Tochilin, Mainach, and Uvuchin). Representative sections of this formation were also studied along banks of large Rassoshina, Polovinka, Snatolveem, Belogolovaya, and Ushkh rivers (Fig. 1). We compiled the detailed lithological columns, studied structural-textural features of sandstone beds and their interrelations, and took samples of all rock varieties.

The *Tochilin section* is located on the Sea of Okhotsk coast. Rocks of this section make up a large anticline, with core composed of sediments of the Snatol Formation. The anticline core is buried under talus, but some fragments are exposed. Rocks of the formation show an almost horizontal bedding (at 5°–7° in some places). The most complete description of this section is given in (Gladenkov et al., 1991). The coastal outcrop shows only the upper (most sandy) part of the Snatol Formation with a total thickness of 400 m. The northeastern limb of the fold is characterized by dip-slip tensile strains (Moiseev and Solov'ev, 2010) and compression with wedging and overthrusting.

Figure 2 shows a summary section of this formation with the designation of sampling sites. In total, more than 50 sandstone samples were taken. Among them,

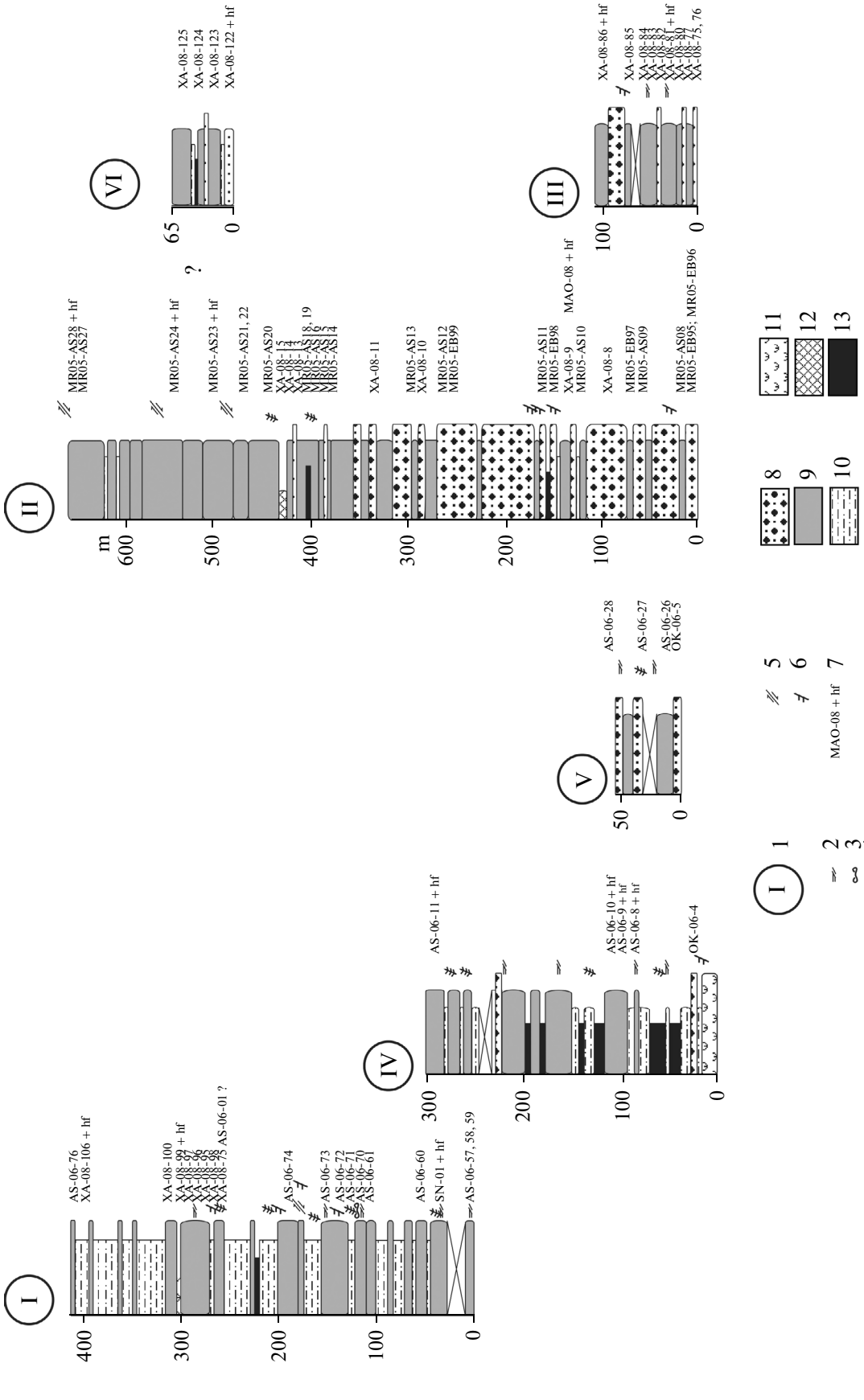

Fig. 2. Lithological columns of the studied sections. (1) Section nos. (see Fig 1): (I) Tochilin, (II) Mainach, (III) Uvuchin, (IV) Rassoshina River, (V) Polovinka River, (VI) Belogolovaya River; (2–6) Structural and textural properties: (2) oblique bedding, (3) fucoids, (4) unified plant detritus, (5) disjunctive dislocations, (6) sharp contact; (7) sample no. (+hf, heavy fraction analyzed); (8–13) lithological composition: (8) conglomerates, (9) sands and sandstones, (10) siltstones and clays, (11) tuffs and cherts, (12) andesite olistolith, (13) coal.

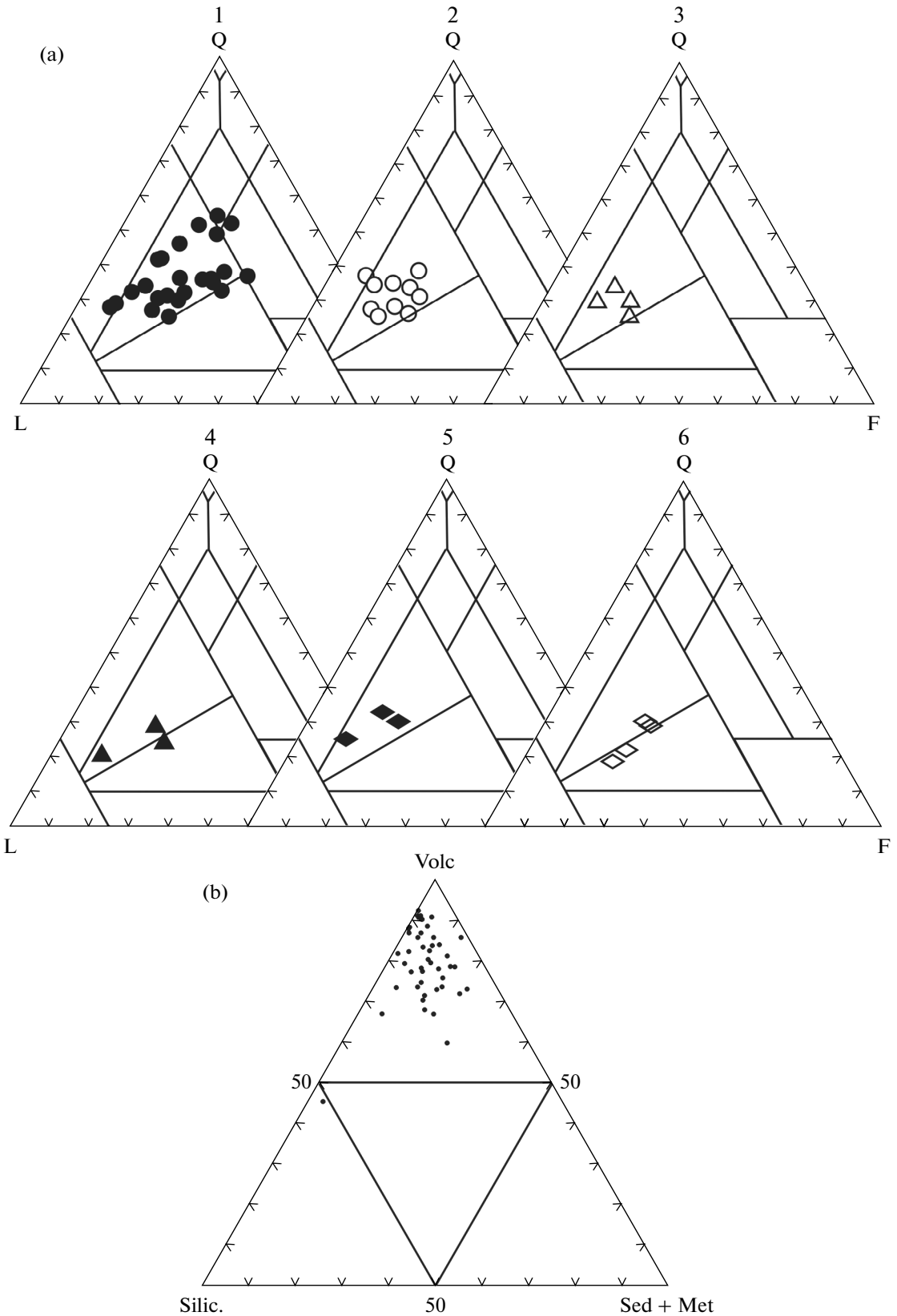

Fig. 3. Sandstone composition, after (Shutov, 1975). (a) (QFL) classification diagram of sandstone composition, Q = Qm + Qp, F = Fm + Fp, L = Qq + Fq + Lv + Lm + Lssh + Lsa + Lsch + Lst + Lso. (1–3) Marine coastal sections: (1) Tochilin, (2) Mainach, (3) Uvuchin; (4–6) sections along banks of large rivers: (4) Rassoshina River, (5) Polovinka River, (6) Belogolovaya River. (b) Compositional diagram of rock fragments, after (Shvanov, 1987). (volc) Volcanic, (silic) cherts and siliceous shales, (sed + met) sedimentary and metamorphic.

Table 1. Composition of sandstones of the Snatol Formation

Sample	Qm	Qp	Qq	P	Fq	Lv				Lm	Ls						Op	nOp	U	T	Mtx	Aut
						Lvl	Lvm	Lvf	Lvv		Lssh	Lsa	Lss	Lsch	Lst	Lso						
Tochilin section																						
AS-06-57	84	14	34	69	70	0	66	12	18	0	2	0	1	0	0	0	4	1	12	387	129	6
AS-06-59	133	41	20	85	20	0	21	5	23	0	5	0	0	0	0	0	6	4	6	369	94	14
SN01	60	22	5	28	3	10	4	5	30	15	0	0	5	10	0	0	2	2	4	203	88	7
AS-06-60	161	15	8	61	22	0	28	22	20	0	0	0	0	0	0	1	1	6	5	350	110	8
AS-06-61	135	21	5	78	31	0	21	0	5	0	0	0	0	0	0	1	2	6	11	316	112	13
AS-06-69	106	12	3	90	45	0	24	45	0	0	0	0	0	6	0	0	0	7	22	360	130	19
AS-06-70	91	13	12	41	23	0	27	9	88	1	0	0	0	0	0	3	0	2	6	316	96	6
AS-06-72	121	5	4	38	11	0	14	17	70	0	0	15	0	5	0	2	0	5	9	316	107	6
AS-06-73	72	11	21	22	31	0	46	32	56	0	0	12	0	0	0	0	0	2	2	307	105	8
AS-06-75	118	20	8	47	13	0	8	11	56	2	0	11	0	0	0	3	0	9	8	314	92	11
AS-06-76	68	14	8	63	9	25	30	21	15	0	4	0	0	0	0	1	9	4	8	279	89	11
AS-06-01	141	35	7	69	14	0	32	0	20	0	0	0	0	2	0	1	1	4	20	346	98	7
XA-08-98	76	15	8	74	21	13	25	38	16	3	6	5	7	1	0	1	5	3	5	322	130	3
XA-08-97	82	13	14	120	17	14	9	13	20	2	3	6	0	0	0	0	1	0	5	319	154	14
XA-08-99	89	20	11	114	20	25	12	12	25	5	0	4	0	0	0	0	4	5	2	348	65	5
XA-08-100	91	17	8	94	13	30	15	16	24	0	0	0	0	0	0	2	5	7	4	326	86	7
XA-08-101	74	12	15	57	7	30	35	26	22	0	0	0	0	0	0	1	10	5	4	298	88	7
XA-08-102	81	27	13	63	3	27	19	33	15	0	15	1	0	0	0	2	19	2	3	323	93	9
XA-08-103	68	17	15	83	10	16	19	56	48	0	11	0	0	0	0	3	7	6	4	363	54	10
XA-08-104	82	11	27	31	9	32	25	26	37	1	7	2	0	0	0	1	13	1	4	309	79	10
XA-08-105	57	16	11	21	5	17	32	70	12	0	15	0	0	0	0	0	4	0	5	265	100	9
XA-08-106	69	36	17	86	5	28	7	9	26	0	10	0	0	0	0	0	5	5	8	311	117	9
XA-08-107	70	20	25	55	13	37	35	15	10	0	9	7	0	0	0	3	11	3	4	317	119	12
XA-08-110	78	17	22	46	9	12	13	20	27	0	6	0	0	0	0	0	15	7	4	276	105	12
XA-08-113	44	10	3	92	5	21	11	22	34	0	15	0	0	0	0	0	7	4	5	273	87	7
XA-08-114	78	11	8	83	12	12	16	23	37	0	7	0	0	0	0	0	15	2	3	307	103	8

Table 1. (Contd.)

Sample	Qm	Qp	Qq	P	Fq	Lv				Lm	Ls						Op	nOp	U	T	Mtx	Aut
						Lvl	Lvm	Lvf	Lvv		Lssh	Lsa	Lss	Lsch	Lst	Lso						
Mainach section																						
MR-05AS08	53	15	16	46	15	10	23	45	10	10	6	0	5	0	0	0	5	3	11	263	115	19
MR-05EB97	51	13	14	44	9	18	35	32	16	5	2	0	10	0	0	0	6	3	16	274	121	9
XA-08-8	74	13	20	62	23	25	41	19	5	9	0	0	13	0	0	0	4	4	5	317	98	16
MR-05AS15	74	23	8	61	8	15	18	40	11	11	4	0	11	0	0	0	8	2	8	302	101	11
XA-08-13	97	15	2	90	0	2	67	41	22	13	0	0	7	0	0	0	3	5	4	368	116	8
XA-08-14	86	38	12	58	9	15	42	21	57	5	0	0	7	0	0	0	5	5	7	367	100	6
MAO-08	45	20	6	61	2	15	23	29	39	5	0	0	0	0	0	0	37	5	5	292	107	10
MR-05AS23	89	21	26	25	38	0	24	14	29	4	0	4	0	0	0	18	1	4	4	301	112	21
MR-05AS24	96	29	13	68	30	16	10	14	32	2	5	0	0	1	0	4	0	2	13	335	97	16
MR-05AS28	68	31	19	34	19	20	12	39	22	8	2	0	0	4	0	5	0	25	8	316	103	13
Uvuchin section																						
XA-08-80	68	10	10	75	14	15	32	43	20	0	0	0	13	7	0	2	5	6	7	327	51	6
XA-08-81	76	12	15	41	17	19	36	26	32	0	0	0	15	8	0	0	5	9	4	315	47	11
XA-08-83	77	18	8	71	13	16	19	52	10	2	5	0	17	5	0	6	7	11	3	340	67	7
XA-08-86	67	24	12	43	5	3	9	31	56	0	7	0	4	6	0	0	9	11	5	292	85	5
Section along the Rossoshina River																						
06AS-08	69	41	37	48	7	13	19	27	15	2	9	0	0	0	0	0	0	8	12	307	108	8
06AS-09	74	31	43	56	4	15	17	34	10	1	7	0	0	0	0	0	0	4	8	304	98	5
AS-06-10	57	16	10	20	8	16	2	15	26	10	4	0	8	13	0	0	0	0	3	208	63	17
AS-06-11	67	20	24	66	15	10	26	34	30	1	4	0	1	0	0	0	5	1	7	311	91	13
Section along the Polovinka River																						
AS-06-26	70	12	35	63	2	15	33	20	15	0	2	0	0	0	1	4	0	6	11	289	53	7
AS-06-27	61	33	20	51	5	19	27	43	22	0	0	0	5	0	0	0	5	6	5	302	77	9
AS-06-28	53	19	13	36	12	40	23	57	31	0	0	0	3	0	0	0	10	3	3	303	68	15
Section along the Belogolovaya River																						
XA-08-122	62	21	12	80	11	15	31	38	17	0	1	0	1	0	0	3	4	3	9	308	59	6
XA-08-123	46	13	17	68	2	19	46	53	10	0	0	0	1	0	0	0	4	2	6	287	99	9
XA-08-124	70	18	14	75	7	20	32	40	15	0	0	0	5	0	0	0	3	4	4	307	121	10
XA-08-125	38	14	12	66	7	25	51	57	16	0	0	0	1	0	0	0	4	2	7	300	150	11

(Qm) Monocrystalline quartz; (Qp) polycrystalline quartz; (Qq) quartzites; (P) feldspars; (Fq) quartz–feldspar intergrowths; rock fragments: (Lv) volcanics, (Lvl) lathlike volcanics (mainly basic and intermediate composition), (Lvm) microlithic volcanics (mainly andesites, dacites, and analogues), (Lvf) felsitic volcanics, (Lvv) crystallized volcanic glass, (Lm) metamorphic rocks, (Ls) sedimentary rocks, (Lssh) clays, (Lsa) mudstones and siltstones, (Lss) fine-grained sandstones, (Lsch) cherts, (Lst) tuffs and tuffogenic mudstones, (Lso) other sedimentary rocks (carbonates, coal), (Op) ore minerals, (nOp) colored minerals, (U) intensely altered minerals; (T) total grains calculated in the thin section, (Mtx) matrix and cement, (Aut) authigenic minerals.

relationship between the major minerals and rock clasts were examined in 23 thin sections. In terms of composition, the studied sandstones can be assigned to the group of quartz–feldspar graywackes. Some samples represent the mesomictic and arkosic sandstones according to the classification by V.D. Shutov (1975).

In general, the sandstones are composed of the mono- and polycrystalline quartz (often well-rounded) grains with tiny fluid inclusions. Quartz and feldspar intergrowths are subordinate. Feldspars are represented by the major plagioclases and the less common platy or irregular microclines and orthoclases (often twinned). Feldspars are replaced by sericite (carbonate in some places). Rock clasts are mainly represented by the lathlike and felsitic volcanic rocks. Quartzite and sedimentary rock clasts are less common. Metamorphic rock clasts are virtually missing (Fig. 3).

The *Mainach section* is located on the Sea of Okhotsk coast near the Babushkin Cape. The section is confined to the western limb of a monocline (Fig. 1) dipping at 30°–40° near the contact of Middle Eocene and Upper Cretaceous rocks. It flattens toward the central part of the fold down to 10°–15°. The basement here is represented by sandstones of the Mainach Formation of the distal turbidite facies (Solov'ev, 2008) accumulated in the deep-water environment. They are underlain with angular and stratigraphic unconformity by rocks of the Snatol Formation. Direct contact between them is buried under debris, and the beach shows Cenozoic andesite boulders up to 2 m in diameter. Olistolith of the petrographically similar andesite from sandstones of the Snatol Formation, which was found 30 m upward the section, was dated by the K–Ar method at 87 ± 3.5 Ma corresponding to the Coniacian–Santonian interval (Khisamutdinova et al., 2015). The lower part of the sequence is composed of variegated different-pebble conglomerates. Their age and composition are given in (Khisamutdinova et al., 2015). They are replaced upsection by shallow-marine sandstones. The sandstone-dominated Snatol Formation includes interbeds of coaliferous clayey rocks (Fig. 2).

The structural-textural pattern of sandstones (abundance of ripple marks and oblique bedding emphasized by the distribution of coaliferous particles) suggests their deposition in a shallow-water environment. The sandstones often contain ferruginated zones. In terms of composition, the sandstones correspond to feldspar–quartz graywackes, and the content of quartz (mono- and polycrystalline varieties) is 25–37%. Clasts are represented by quartzite grains that can be defined as rock clasts. Feldspars are represented mainly by plagioclases, with the subordinate K-feldspars (orthoclase, microclines) accounting for 8–24%. They are observed usually as platy grains and less commonly as unrounded crystals. Secondary alterations (sericitization and carbonatization) are irregular. Rock clasts are dominated by the volcanic (felsitic and microlithic) rock varieties and the volcanic (often devitrified and chloritized, but sometimes zeolitized) glasses. Sedimentary rocks (sandstones and clayey fragments) are much less common. Clasts of metamorphic rocks (chlorite and amphibole schists) are rare (Fig. 3).

The *Uvuchin section* is exposed on the cliff at the Kvachin Bay (Fig. 1). Rocks in this section make up two folds. The anticline is represented by a large outcrop with Cretaceous sandstones in the core. The conjugated NNW-oriented syncline, which includes Miocene rocks in the core, dips at 17°–25°. Here, the Paleogene portion of the sedimentary section is appreciably reduced. Thickness of the Snatol Formation is 72 m (Fig. 2). Rocks of this formation lie with angular and stratigraphic unconformity on the Upper Cretaceous sandstones of the Mainach Formation. The lower part of the sequence is mainly composed of conglomerates alternating with sandstones. The conglomerates make up variegated and different-pebble interbeds up to 50–70 cm thick. The sandstones, which alternate with conglomerates, are coarse- and medium-grained (often oblique-bedded) rocks with "floating" pebbles. The composition and age of pebbles in conglomerates from the lower part of the section are scrutinized in (Khisamutdinova et al., 2015).

In terms of composition, the sandstones correspond to feldspar–quartz graywackes (Fig. 3). Quartz (mono- and polycrystalline varieties without fluid inclusions) make up 23–31% of the thin section area. In some places, they include triangular quartz grains with smooth edges and moderate roundness suggesting their volcanic origin. Feldspars are represented by plagioclases, and K-feldspars are rare. Platy and quadrate feldspar grains make up 13–22% of the thin section area. Feldspars are replaced in some places by aggregates of saussurite (sericite in rare cases). Rock clasts are commonly represented by volcanic glass and volcanic rocks with the felsitic and microlithic groundmass. Volcanic glasses are partly devitrified, replaced by clay mineral aggregates, or chloritized. Volcanic rock fragments have a fresh appearance, although the vitreous mass in interstices between plagioclase laths and crystals are often replaced by secondary clay minerals. Volcanic rock clasts are characterized by moderate and high roundness, and they are usually larger than mineral grains in sandstones. In addition to volcanic rocks, clasts of probably Late Cretaceous sandstones are significant.

The *Rassoshina River section*, which is exposed on the right bank of the river 800 m upward its inflow into the Napan River, comprises rocks of the Khulgun (?) and Napan formations (*Karta* ..., 1999) (Fig. 1). They lie with a sharp angular unconformity over Late Cretaceous (?) volcanic rocks. We combined the description and comparison of sandstones of this section with sandstones in the stratotype coastal sections, because one can see here a distinct contact of the lower part of

the sequence and the Upper Cretaceous basement. Therefore, we can compare confidently sandstone beds located at one stratigraphic level. The basal part of the Cenozoic section is composed of the low-sorted conglomerates (with siltstone interbeds) grading upsection into siltstones (with large coal seams) (Fig. 2) and further 15 m upsection into the coarse-grained sandstones. The siltstones include abundant coalified plant detritus and flora imprints. The sandstones are also saturated with the coalified plant detritus on the bedding surface, emphasizing the oblique bedding. In terms of grain size composition, the sandstones grade from the coarse-grained to the fine-grained variety. The fine-grained sandstones are more mature and marked by the absence of plant detritus. Apparent thickness of the sandstone sequence is 130 m. In the classification diagram (Shutov, 1975), data points of sandstones are mainly clustered in the graywacke domain (Fig. 3). Quartz occurs as fresh, rounded and angular (sometimes polycrystalline) grains (19–27%) with rare fluid inclusions. Feldspars (12–24%) mainly represented by plagioclases make up mono- and polysynthetically twinned crystals. They are weakly rounded and partly replaced by secondary minerals (sericite, carbonate). The sandstones are mainly composed of volcanic and sedimentary rock fragments (46–62%). The felsitic effusive rocks account for up to 10% of the clastic particles. The subordinate component is represented by volcanic glass, felsitic and microlithic volcanic rocks, and sandstones.

The *Polovinka River section* is located on the left bank of the river flowing from Mt. Polovinnaya (Fig. 1). The exposure is composed of rocks of the Napan Formation (*Karta* ..., 1999). It includes a horizontal sandy sequence with an apparent thickness of about 60 m. The sequence base is unexposed. The lower part of the section comprises the friable fine-pebble conglomerates cemented with brown sandstone (Fig. 2). The conglomerates are replaced upsection by sandstones with abundant "floating" coal pebbles, horizontal and oblique bedding, and coalified plant detritus. The section top includes a thin conglomerate interbed giving way to glauconite sandstones.

Sections exposed at the Polovinka and Napan rivers are characterized by similar compositions and appearance of sandstones, as well as the presence of coal seams. We believe that sandstones exposed on cliffs along the Polovinka River correlate with the middle sandy section along the. Rassoshina River.

Sandstones from the Polovinka section correspond to the feldspar–quartz graywackes (Fig. 3). Quartz (13–23%) occurs as subrounded and well-rounded monocrystalline grains. Triangular grains observed in some places suggest the disintegration of volcanic rocks. Feldspars (11–21%) are represented by subrounded grains and elongated crystals of plagioclase and microcline that are altered by sericite. Quartz and feldspar intergrowths are likely fragments of felsic rocks.

The *Belogolovaya River section* located considerably southward from the sections described above is presented here for the sake of comparison. The summary section is compiled from separate sectors exposed on river walls. Apparent thickness of subhorizontal sandstones is 65 m. Since the sequence base is unexposed, we cannot determine the position of sandstones relative to the Cretaceous basement. The sandstones correspond to quartz–feldspar and feldspar–quartz graywackes in the classification diagram. Quartz and feldspars in this section are similar to those in sections exposed along the Rossoshina and Polovinka rivers. Rock clasts in this section include equal amounts of felsitic, lathlike, and microlithic volcanic rocks.

We supplemented the processing of original rock material with the analysis of data in the reports of VNIGRI (L.V. Goma, chief executive; Yu.S. Voronkov, L.M. Pylina, et al., executives) based on the study of core materials from parametric boreholes drilled in the Tigil area. Figure 4 presents the location of boreholes and the composition of sandstones sampled from the core material according to the report "Processing of Parametric Boreholes Drilled in the Tigil Area, Western Kamchatka" (L.V. Goma, chief executive). Sandstones recovered by boreholes Rassoshinskaya, Sredne-Rassoshinskaya, Khromovskaya 1, and Khromovskaya 2 are less mature. They are often assigned to graywackes according to the classification by V.D. Shutov (1975). The major minerals in them are represented by quartz and feldspars; rock clasts, by volcanic rock, volcanic glass, sandstone, siltstone, chert, and feldspar–quartz intergrowths.

On the whole, sandstones of the Middle Eocene Snatol Formation, which are exposed on the surface and recovered by parametric boreholes, have immature composition. In the classification diagram, most sandstones fall into the graywacke domain. Some samples taken from the sequence top belong to the oligomictic and mesomictic sandstones (Figs. 3, 4). The composition variation lacks any distinct lateral/vertical trend.

In the summary triangular diagram with geodynamic settings of the pasammite formation (Dickinson, 1983), the rock composition in provenances (and their geodynamic setting) falls into the field of mixed source, as well as eroded and weakly eroded arcs of the transitional type (Fig. 5).

DISCRIMINANT DIAGRAMS, MATURITY DEGREE, AND GEODYNAMIC SETTING OF ERODED ROCKS–SUPPLIERS OF THE TERRIGENOUS MATERIAL

Reconstruction of the sandstone provenance was corroborated by analysis of the contents of petrogenic oxides in the rock. We applied the diagram proposed in

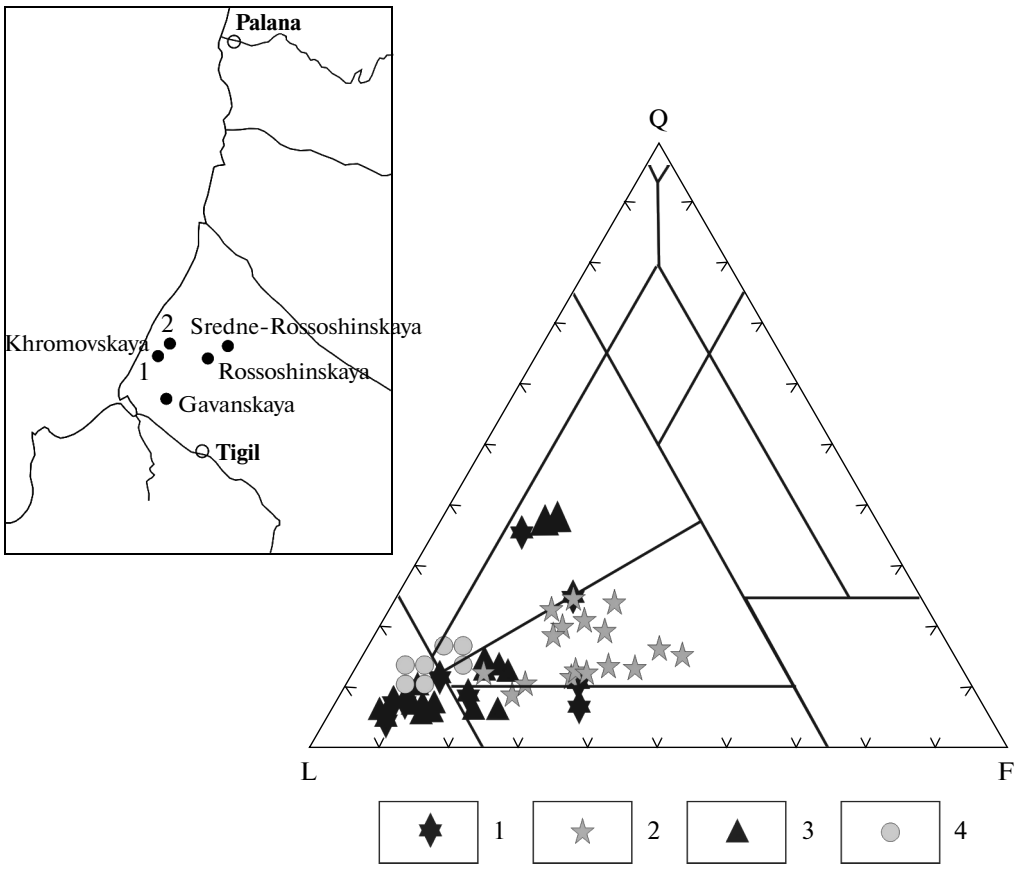

Fig. 4. Composition of sandstones of the Snatol Formation (in cores taken from parametric boreholes in western Kamchatka), after (Shutov, 1975). (QFL) classification diagram of sandstone composition, Q = Qm + Qp, F = Fm + Fp, L = Qq + Fq + Lv + Lm + Lssh + Lsa + Lsch + Lst + Lso. Parametric boreholes: (1) Rossoshinskaya, (2) Khromovskaya 1, (3) Khromovskaya 2, (4) Gavanskaya. Inset shows the location of boreholes.

(Roser and Korsch, 1982) and used often for deciphering provenances of sedimentary basins and tectonic reconstructions (Zhengjun et al., 2005; Concepcion et al, 2012). In this diagram, data points of SiO_2 and (Na_2O + K_2O) in the sandstones (Table 2) fall mostly into the domain of oceanic island arc and partly into the domain of active continental margin (Fig. 6).

With respect to the chemical index of alteration, CIA (Nesbitt and Young, 1984), some data points fall into the domain of unweathered rocks with CIA < 50, while another part falls into the domain with average CIA = 65, which corresponds to slightly altered rocks in the provenance and temperate climate (Fig. 7).

MINERAL COMPOSITION OF THE HEAVY FRACTION

Analysis of the mineral composition of the heavy fraction is essential for deciphering sandstone provenances (Malinovskii and Markevich, 2007; Mange and Otvos, 2005; Morton, 1985; Morton and Hallsworth, 1994, 1999; Morton et al., 2003). We took 18 representative sandstone samples from different sections and examined them thoroughly: preliminary petrographic study, crushing, fractionation, and examination with immersion liquids under a Meiji Techno binocular microscope. The contents of minerals in the heavy fraction of sandstones are given in Table 3.

The heavy minerals were divided conventionally into three assemblages (rock composition indicators) prevailing in the provenance. Such studies were reported previously in (Malinovskii and Markevich, 2007; Mange and Otvos, 2005; Morton et al., 2003; and others). The first (sialic) assemblage is composed of minerals related to the disintegration of felsic intrusive and effusive rocks (zircon, apatite, rutile, and tourmaline). In this assemblage, the major mineral zircon (0.1–34%) is represented by two generations: euhedral colorless (or pale pink) and lilac-pink. The euhedral grains are prismatic (pyramidal in rare cases). Some grains are marked by yellow cathodoluminescence (CL) color. The lilac-pink grains are usually rounded, but some grains are characterized by the prismatic habitus (with smoothed edges) and the lack of CL effect. The grain surface is shiny and smooth, and the luster is vitreous. Rutile, second in abundance

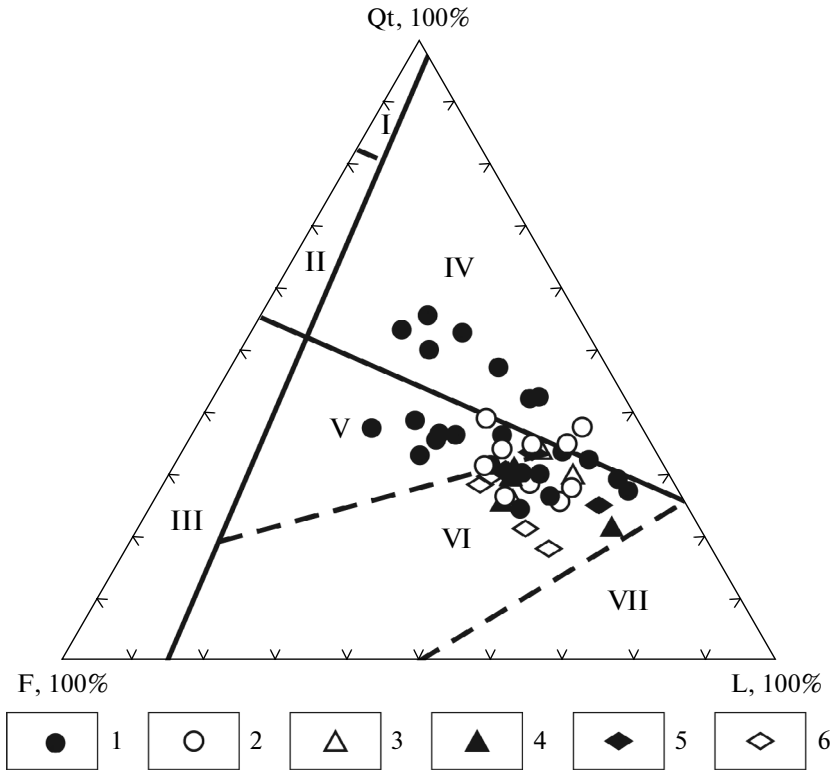

Fig. 5. Composition of sandstones in provenances with various geodynamic settings, after (Dickinson, 1983). (I) Central part of the platform; (II) intermediate zone of the platform; (III) basement projections; (IV) orogenic zones; (V–VII) island arcs: (V) differentiated, (VI) slightly differentiated, (VII) undifferentiated. (1–6) Sections: (1) Tochilin, (2) Mainach, (3) Uvuchin, (4) Rassoshina River, (5) Polovinka River, (6) Belogolovaya River.

(0–20%) in this assemblage, occurs as a black mineral characterized by red (in some cases, red or orange-red) translucence in thin chips and shiny vitreous luster. Irregular (sometimes prismatic) clasts are abundant. Apatite (0–8%) occurs as colorless, transparent, slightly rounded prismatic crystals. Tourmaline (0–0.1%, 14% in one sample) occurs as brown, greenish brown, or dark green rounded and transparent grains.

The second (mafic) assemblage comprises indicator minerals of the major intrusive and effusive rocks (spinel, ilmenite, leucoxene, and pyroxene). The most widespread mineral in the heavy fraction of sandstones is represented by spinel (0–58%) as black splintered grains and well-developed octahedra. The grains have a smooth shiny surface and resinous luster. They are low rounded or subrounded, and the octahedral apex is often smoothed. The assemblage contains nearly equal amounts of leucoxene (0–75%) and ilmenite (0–56%). Leucoxene is marked by beige or gray-beige color and irregular shape. Ilmenite is represented by black, flattened, platy grains with

resinous luster and leucoxenized surface in some places. Pyroxenes (0.1–2%) are subordinate except in one tuffaceous sandstone sample taken near the Ichinsk Volcano that was likely formed during the deposition of the Middle Eocene terrigenous sequence. The content of pyroxenes in this sample is as much as 98%.

The remaining minerals of the heavy fraction and rock fragments from sandstones were united into the third group (anatase, barite, sulfides, ore mineral, amphibole, mica, garnet, and clasts of chlorite and actinolite schists). These minerals can belong to different genetic rock types (igneous, metamorphic, or sedimentary) and, therefore, cannot serve as distinct indicator of rock composition in the provenance. Proportions of these indicator minerals are shown in the summary section (Fig. 8).

We also compiled such columns for the parametric boreholes Rassoshinskaya, Sredne-Rassoshinskaya, Khromovskaya 1, and Khromovskaya 2. The mineralogical data on core material are given in the report (*Otchet* ..., 1986). The columns show a gradual increase of the clastic material derived from the mafic rock source and the simultaneous decrease of minerals of the heavy fraction derived from the felsic rock source. The content of mafic minerals reaches 70%.

Correlation of the summary "terrestrial" section of the Snatol Formation with sections recovered by parametric boreholes makes it possible to define two stages characterized by increase of the discharge of clastic

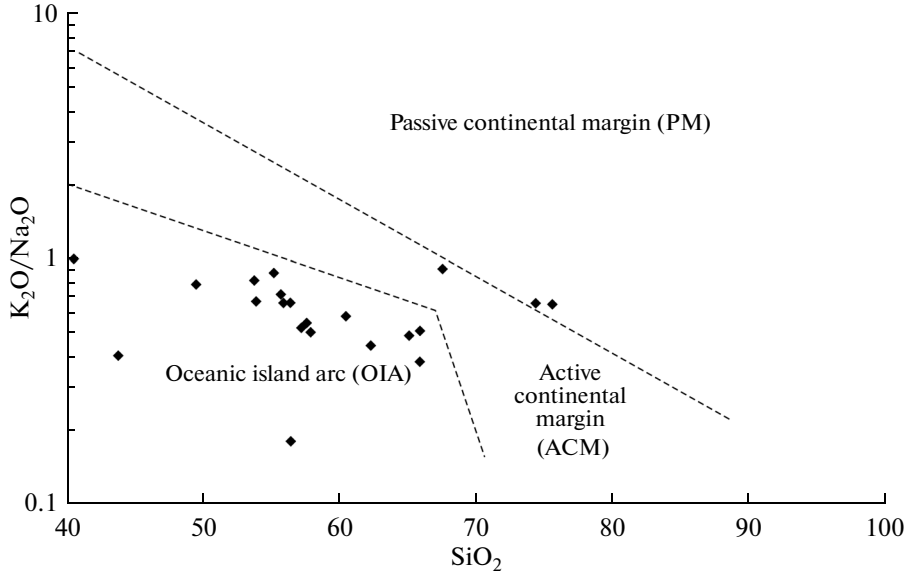

Fig. 6. Data points of sandstone composition in diagram (Roser and Korch, 1986).

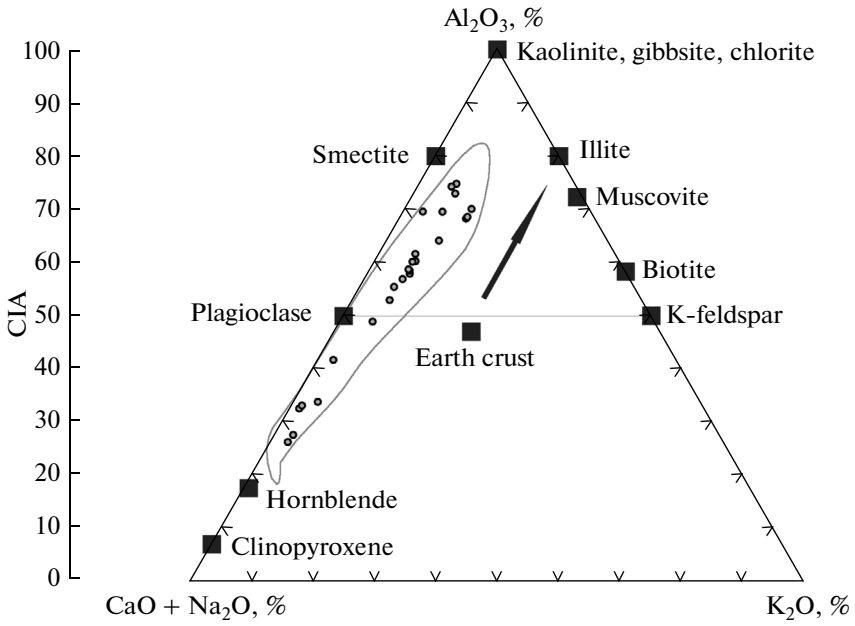

Fig. 7. Data points of sandstone composition in diagram (Nesbitt and Young 1982).

material from felsic rock provenances. The content of indicator minerals of felsic rocks is as much as 38–40% in samples from the terrestrial sections. Variation of their content in core samples from boreholes is as follows: 50% in Khromovskaya 1 and Khromovskaya 2, 39% in Rassoshinskaya, and 63% in Sredne-Rassoshinskaya.

Analysis of the mineral composition of the heavy fraction revealed the existence of at least two Middle Eocene provenances that delivered the clastic material to WKSB. Discharge of terrigenous material from the mafic source rocks was the dominant process, while the discharge from provenances mainly composed of felsic rocks was subordinate.

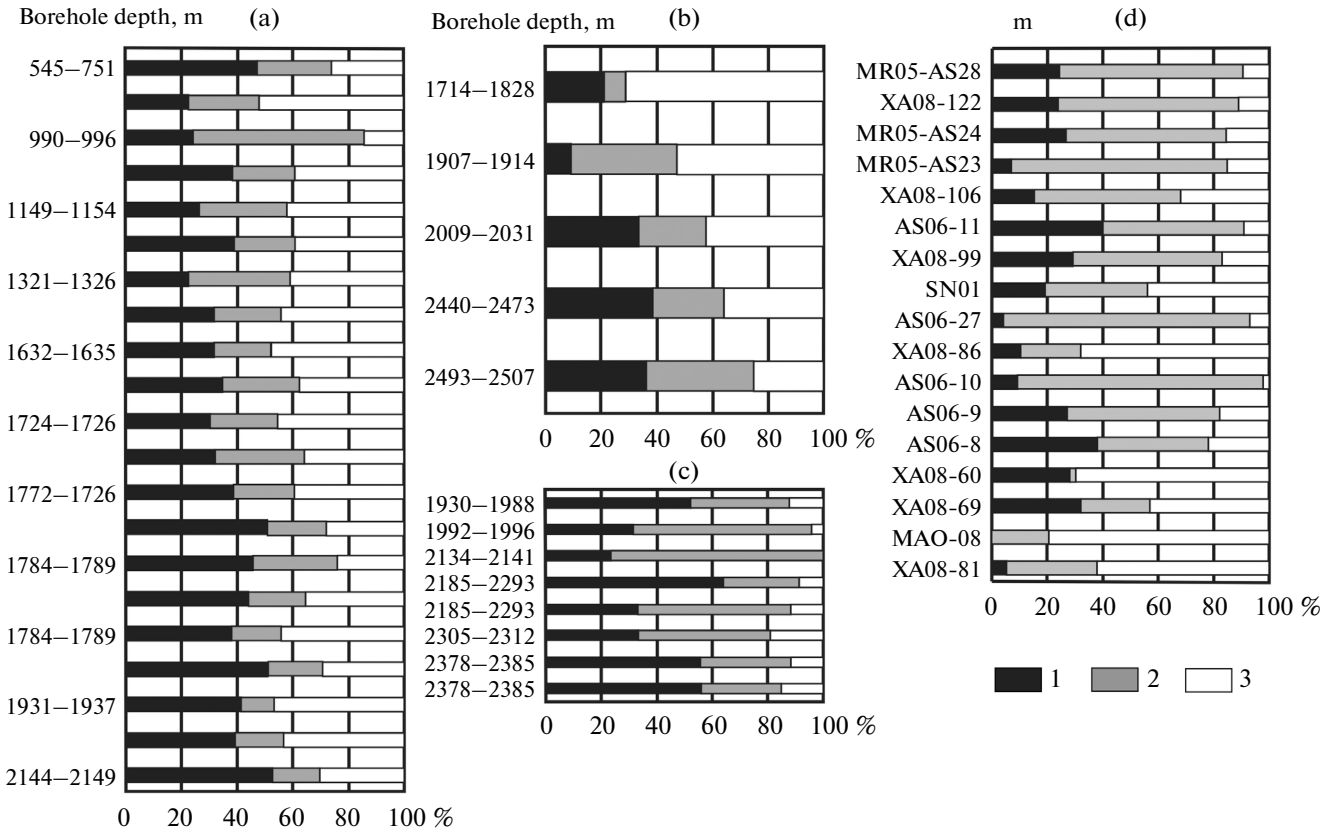

Fig. 8. Distribution of heavy fraction minerals (indicators of eroded rocks) in the studied boreholes and summary column. (a–c) Boreholes: (a) Khromovskaya 1 and Khromovskaya 2, (b) Rassoshinskaya, (c) Sredne-Rassoshinskaya, (d)) summary column of the Snatol Formation (outcrops). (1) Zircon, apatite, rutile, and tourmaline (indicators of the erosion of felsic rocks); (2) spinel, ilmenite, leucoxene, and pyroxene (indicators of the erosion of mafic felsic rocks). (3) garnet, amphibole, anatase, sulfides, and barite (heterogeneous minerals).

MORPHOLOGY OF CRYSTALS AND U–Pb ISOTOPE AGE OF THE CLASTIC ZIRCON

Detailed examination of the detrital zircon included the study of morphology grains and their LA-ICP-MS dating.

Morphology of clastic zircon crystals. We studied the –0.07 mm fraction, which is most representative for the comparison of crystalline forms of zircon. The samples contained two zircon generations: (i) rounded and subrounded grains and short-prismatic crystals with smoothed crimson and deep pink apices and edges; (ii) euhedral colorless and slightly colored crystals of different morphotypes. Crimson grains are extremely rare. Therefore, only colorless grains were counted. In all samples, the average approximate content of grains is as follows (%): countable (nonrounded) grains 35%, semirounded 45%, and rounded 20%.

Classification of zircon types in (Pupin, 1980) was modified for the convenience of calculation. Morphotypes with similar setting were united into groups without the consideration of elongation coefficient. Designation of each group was based on the extreme left morphotype in the classification. Example of the obtained morphotype distribution for sample SN-01 is given in Fig. 9. Counting was based on 100–250 grains depending on the zircon content in sample. The results showed that the samples are dominated by five zircon morphotypes (H, L4, S9, S15, and S25). Crystal morphotype H is characteristic of the high-alumina muscovite-bearing granites (s-type); morphotype L4, for the hybrid (contaminated) monzonites and alkaline granites; morphotype S9, for the contaminated subalkaline and alkaline granites; morphotype S15, for the subalkaline and alkaline granites (i-type); and morphotype S25, for the alkaline granitoids and tholeiitic granites (i-type) (Belousova et al., 2006). The content of other zircon morphotypes is extremely low. Detailed data on the morphology of clastic zircon crystals from Middle Eocene sandstones are presented in (Rozhkova et al., 2012).

Thus, the Middle Eocene source of clastic material transported to WKSB was composed of the dominant subalkaline (calc-alkaline) granitoids and the subordinate high-alumina muscovite granites. Correlation of the zircon crystal morphology with the formation con-

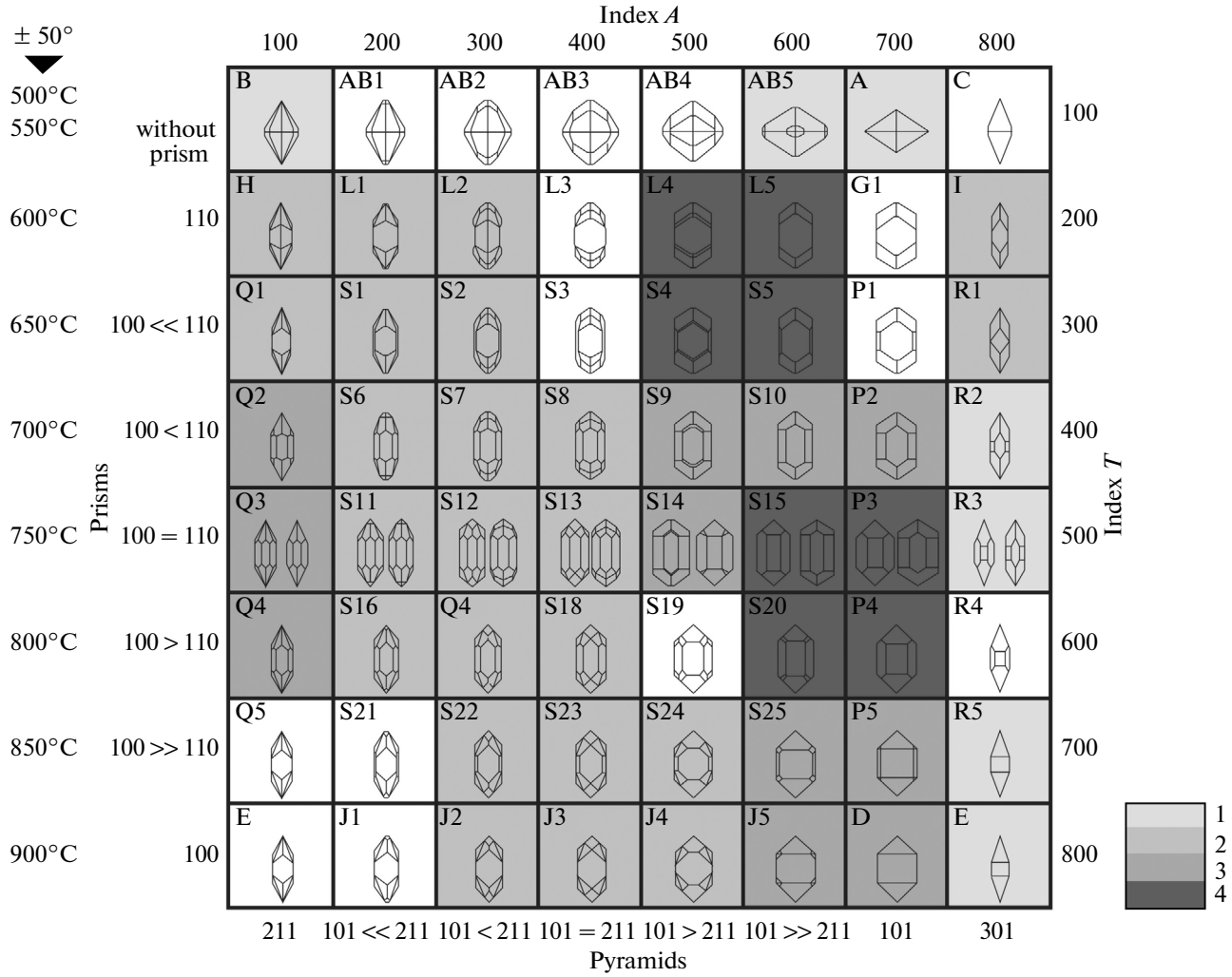

Fig. 9. Classification of zircon crystal morphotypes depending on their formation temperature (Pupin, 1980). (Index A) Al/(Na + K) ratio controlling the development of zircon pyramids; (index T) parameter affecting the development of zircon prisms. (1–4) Content of clastic zircon crystals of different morphologies in the sandstone sample SN-01, %: (1) 0.1–1, (2) 1.1–5, (3) 5.1–10, (4) 20.1–25.

dition and granite type (Belousova et al., 2006) is shown in Fig. 10.

The U–Pb isotope dating of clastic zircons was accomplished for two samples: sample SN-1 from the lower part of the Tochilin section (Fig. 2, I) and sample AS-06-10 from the section exposed in the Rassoshina River valley (Fig. 2, VI). Sample SN-1 occurs above sample AS-06-10 in the stratigraphic setting. Zircon monofractions were separated from these samples. During preparation of the laboratory cartridge, clastic zircon grains were spread in rows upon the two-sided adhesive tape using a stencil plate. Crystals of standard SL2 with an age of 563 Ma (Gehrels et al., 2008) were placed at the cartridge center. Then, the cartridge surface with zircon grain was polished. Cathodoluminescence images of the samples were obtained with a JEOL JSM 5600 scanning electron microscope equipped with CL detector (Microanalytical Center of Stanford University). The U–Pb dating was carried out by the LA-ICP-MS method at the Arizona Laser Chron Center (Tucson, United States) (Gehrels, 2011; Gehrels et al., 2008).

Dating was accomplished for 100 grains in each sample. Grains without fluid inclusions and visible distortions were chosen based on CL images for the isotope dating. Zircon ablation was carried out in a New Wave UP193HE Excimer Laser (wavelength 193 nm, crater diameter 30 μm). Isotopes of U, Th, and Pb were measured simultaneously in the following way: 15 s–one measurement with the laser off); 15 s–laser ablation and 30-s delay for the preceding sample clean-up and preparation of the next analysis. The crater ablation depth was ~15 μm. For each analysis, error in the determination of $^{206}Pb/^{238}U$ and $^{206}Pb/^{204}Pb$ was not higher than ~1 or 2% (±2σ). Error in the determination of $^{206}Pb/^{207}Pb$ and $^{206}Pb/^{204}Pb$

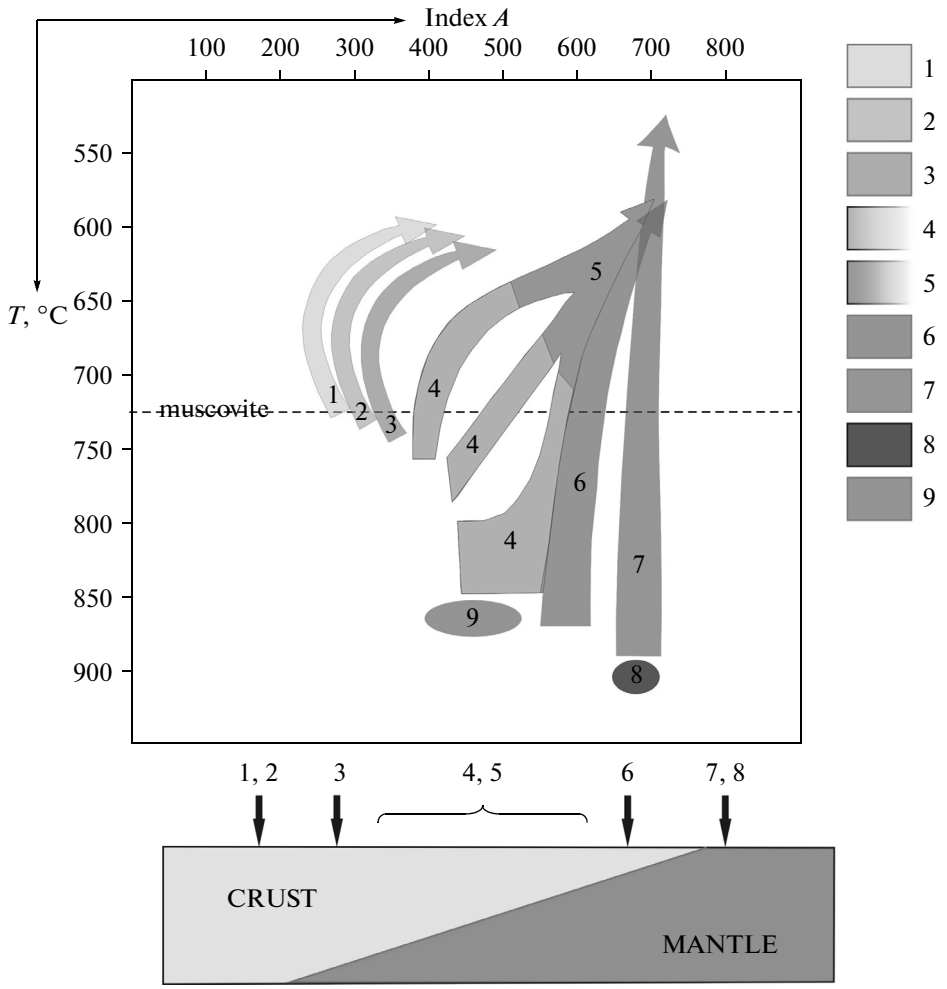

Fig. 10. Correlation of the morphology of zircon crystals with the petrogenetic setting of host granites, after (Belousova et al., 2006). (1–3) Calc-alkaline series: (1) high-alumina leucogranites, (2) intrusions of high-alumina monzogranites and granodiorites, (3) subautochthonous monzogranites and granodiorites; (4–6) crustal–mantle granites: (4) granodiorites and monzonites, (5) monzogranites and high-alumina granites, (6) granites of the subalkaline series; (7–9) mantle granites: (7) alkaline series, (8) tholeiitic series, (9) charnockites.

was not also higher than ~1 or 2% (±2σ) for most grains, less than 1% for the grains with an age of more than 1 Ga, and higher than the above values for younger grains due to low intensity of Pb signal. Concentrations of U and Th were calibrated relative to the zircon standard SL2 (Gehrels et al., 2008) containing 518 ppm U and 68 ppm Th. The analysis was only based on concordant grains, i.e., grains with discordance less than 10%. Concordia plots were drawn based on the ISOPLOT program (Ludwig, 2003).

Dating of the clastic zircon revealed that the studied sandstones contain different-age zircons (Fig. 11). The samples include a significant amount (22–33%) of Precambrian zircon grains with a prominent peak at 2.0–1.8 Ga. Paleozoic zircon grains are rare (5–11%) and make up a significant peak at 496 Ma only in sample 06AS-10. Much more abundant are Mesozoic grains (52–68%) with a peak at 118–70 Ma. Cenozoic zircons are also present (4 to 5%).

In Fig. 11, clastic zircons from Paleogene terrigenous sediments of the Ukelayat flysch (Solov'ev, 2008) and recent sand of the Amur River (Safonova et al., 2010) are compared. All samples from the Sea of Okhotsk region contain rare Archean zircon grains, whereas grains with an age of 2.0–1.8 Ga make up a significant peak (14–33%). Their content is lower (8%) only in sediments of the Amur River. The Early Proterozoic zircon was likely derived from rocks of the Siberian Craton or blocks related with Siberia (Avekov, Okhotsk, and Omolon), where magmatic activity was maximal about 1.9 Ga ago (Rosen, 2002). Recent studies revealed the continental crust formation 2.0–1.8 Ga ago during the formation of supercontinent Columbia (Safonova et al., 2010). The Paleozoic zircon is insignificant. The Mesozoic (~250–66 Ma) zircon is most abundant (~52–74%). Zircon older than 110 Ma is abundant only in sediments of the Amur River (~47%). Its content is appreciably lower (~10–

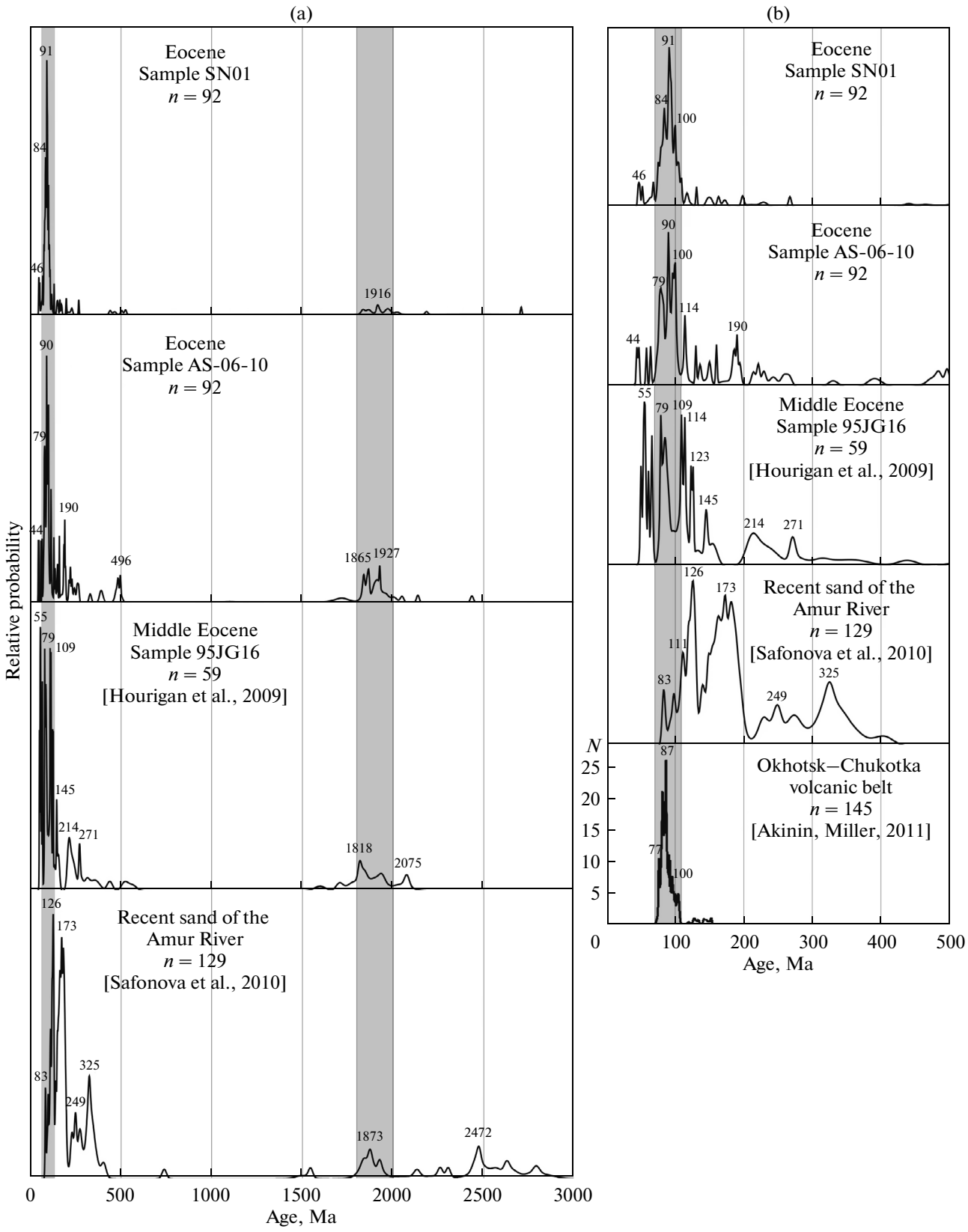

Fig. 11. Distribution of the clastic zircon age. (a) Interval 0–3500 Ma, (b) interval 0–500 Ma, (n) number of analyzed grains.

Table 2. Chemical composition of sandstones of the Snatol Formation (wt %)

Sample no.	Section, formation	SiO_2	TiO_2	Al_2O_3	Fe_2O_3	FeO	MnO	MgO	CaO	Na_2O	K_2O	P_2O_5	L.O.I.	Total	H_2O^-	CO_2	H_2O^+
Marine sections																	
AS-06-01	Tochilin section, sn	57.91	0.80	17.71	2.01	5.18	0.04	3.97	1.75	2.81	1.40	0.16	5.64	99.38		1.09	
AS-06-57	″	56.45	2.98	12.34	3.64	6.67	0.04	5.14	1.83	3.02	0.54	0.13	6.50	99.28		1.22	
AS-06-59	″	53.77	0.88	15.66	1.78	4.58	0.15	3.40	6.52	2.10	1.70	0.14	8.81	99.49		4.48	
AS-06-61	″	56.42	0.95	16.99	3.23	3.39	0.07	3.52	3.57	2.33	1.53	0.16	7.07	99.23		2.49	
AS-06-70	″	55.72	0.88	14.60	2.18	2.22	0.14	2.33	8.99	2.32	1.65	0.17	8.86	100.06		5.27	
AS-06-71	″	53.90	1.00	16.21	2.11	5.02	0.16	3.51	6.25	2.30	1.53	0.17	7.75	99.91		4.97	
AS-06-72	″	49.50	0.92	14.62	2.36	3.36	0.20	2.50	11.70	2.00	1.56	0.18	10.79	99.69		7.51	
AS-06-73A	″	55.91	0.89	15.04	2.28	3.37	0.12	2.96	7.30	2.47	1.62	0.15	8.16	100.27		4.91	
AS-06-73B	″	57.62	0.71	13.44	2.20	3.96	0.09	3.09	7.04	2.43	1.32	0.16	7.46	99.52		4.59	
AS-06-74	″	37.08	0.89	14.54	2.23	2.48	0.11	2.27	16.85	2.59	0.85	0.11	19.38	99.38		10.72	
AS-06-75	″	55.20	0.90	15.80	2.67	3.02	0.10	2.91	7.50	2.13	1.85	0.15	8.00	100.23		5.19	
XA-08-111	″	40.53	0.61	10.77	1.51	2.18	0.21	2.04	18.57	1.24	1.23	0.11	20.25	99.25	0.92	16.12	3.14
XA-08-114	″	62.33	0.81	13.91	2.85	1.66	0.04	1.54	4.59	3.21	1.41	0.10	7.25	99.70	1.12	3.58	2.52
MR-05-AS-23	Mainach section, sn	35.91	0.46	7.95	5.85	3.91	0.19	3.51	19.19	2.25	0.83	0.56	19.00	99.61		13.13	
MR-05-AS-24	″	43.78	0.53	9.74	1.28	1.47	0.17	1.52	21.84	2.60	1.04	0.06	15.50	99.53		11.78	
MR-05-AS28	″	67.60	0.52	10.55	4.23	2.66	0.03	1.86	1.40	1.84	1.66	0.08	6.94	99.37		0.20	
XA-08-13	″	65.14	1.15	13.46	2.85	2.43	0.04	1.94	2.09	3.67	1.77	0.09	4.80	99.43	0.95	1.07	2.05
XA-08-71	″	57.22	0.75	14.77	1.58	4.13	0.18	1.79	5.70	3.14	1.63	0.20	8.74	99.83	1.10	4.47	3.16
Sections along the bank of large rivers																	
AS-06-09	Rossoshina River, np	34.44	0.47	9.90	3.49	4.15	0.15	5.00	18.50	1.52	0.45	0.11	21.24	99.42		19.37	
AS-06-11	″	60.50	0.60	12.99	1.42	3.11	0.20	2.50	5.41	2.35	1.36	0.17	8.90	99.51		5.77	
AS-06-26	Polovinka River, np	34.25	0.50	10.20	3.19	4.46	0.14	4.90	18.44	1.62	0.50	0.09	20.93	99.22		18.14	
AS-06-27	″	65.93	0.50	17.00	1.10	1.99	0.04	0.87	2.21	2.44	1.23	0.14	6.60	100.05		3.28	
AS-06-28	″	65.92	0.79	13.77	2.72	3.87	0.03	2.98	0.53	3.31	1.25	0.19	3.88	99.24		0.20	
XA-08-123	Belogolovaya River, sn	74.44	0.45	12.72	1.47	1.05	0.02	0.98	0.50	2.98	1.95	0.10	3.05	99.71	1.00	0.22	1.84
XA-08-125	″	75.66	0.44	10.86	3.07	0.54	0.09	0.97	0.62	2.64	1.71	0.12	2.96	99.68	0.81	0.22	2.01

Formations: (sn) Snatol, (np) Napan, (–"–) section and formation as in the previous row.

Table 3. Contents of minerals of the heavy fraction (%) in samples of the Snatol sandstone (samples are ordered from the section bottom to top)

Sample no.	Zircon	Rutile	Apatite	Garnet	Tourmaline	Sulfides	Amphibole	Pyroxene	Anatase	Spinel	Ilmenite	Leucoxene	Barite	Epidote	Black ore
MR-05-AS-28	5	11	8	9	0	0.5	0	0	0	58	0	7	0	0	0
XA-08-132	0.2	0	0.8	0.01	0	0.5	0.01	98	0	0	0	0	0	0	0
XA-08-122	11	13	0	11	0	0.1	0.1	1	0	8	16	40	0	0	0
MR-05-AS-24	13	9	4.5	8	0	7	0.5	0	0	7	22	29	0	0	0
MR-05-AS-23	4	3	0	14	0	1	0	5	0	1	56	16	0	0	0
XA-08-106	11	4	0	12	0	20	0	0	0	17	10	26	0	0	0
AS-06-11	17	9	0	9	14	0	0	8	0	1	41	1	0	0	0
XA-08-99	24	3	2	10	0.1	7	0	0.1	0.1	15	0	39	0	0	0
SN-01	17	2	0.1	10	0	1	0	2	0	12	10	13	0	0	33
AS-06-27	1	2	0	1.5	1	0.5	0	0	0	25	1	63	5	0	0
XA-08-86	3	2	5	1	0	67	0	0.1	0.1	0	21	1	0	0	0
AS-06-10	4	4	1	2	0	0	0	0.1	0.1	14	0	75	0	0	0
AS-06-09	22	4	0.1	18	1	0	0.1	0	0	26	0	29	0	0	0
AS-06-08	34	4	0	8	0	14	0	0.1	0.1	21	4	15	0	0	0
XA-08-60	8	20	0	2	0	63	5	2.1	0	0.1	0	0	0	0	0
XA-08-69	29	3	0	7	0.1	36	0	0	0	3	6	16	0	0	0
MAO-08	0.1	0	0.1	1	0	74	3	1	0.1	2	16	1	0.5	1	0
XA-08-81	3	2	0	2	0.1	60	0.1	0	0.1	0.1	9	24	0	0	0

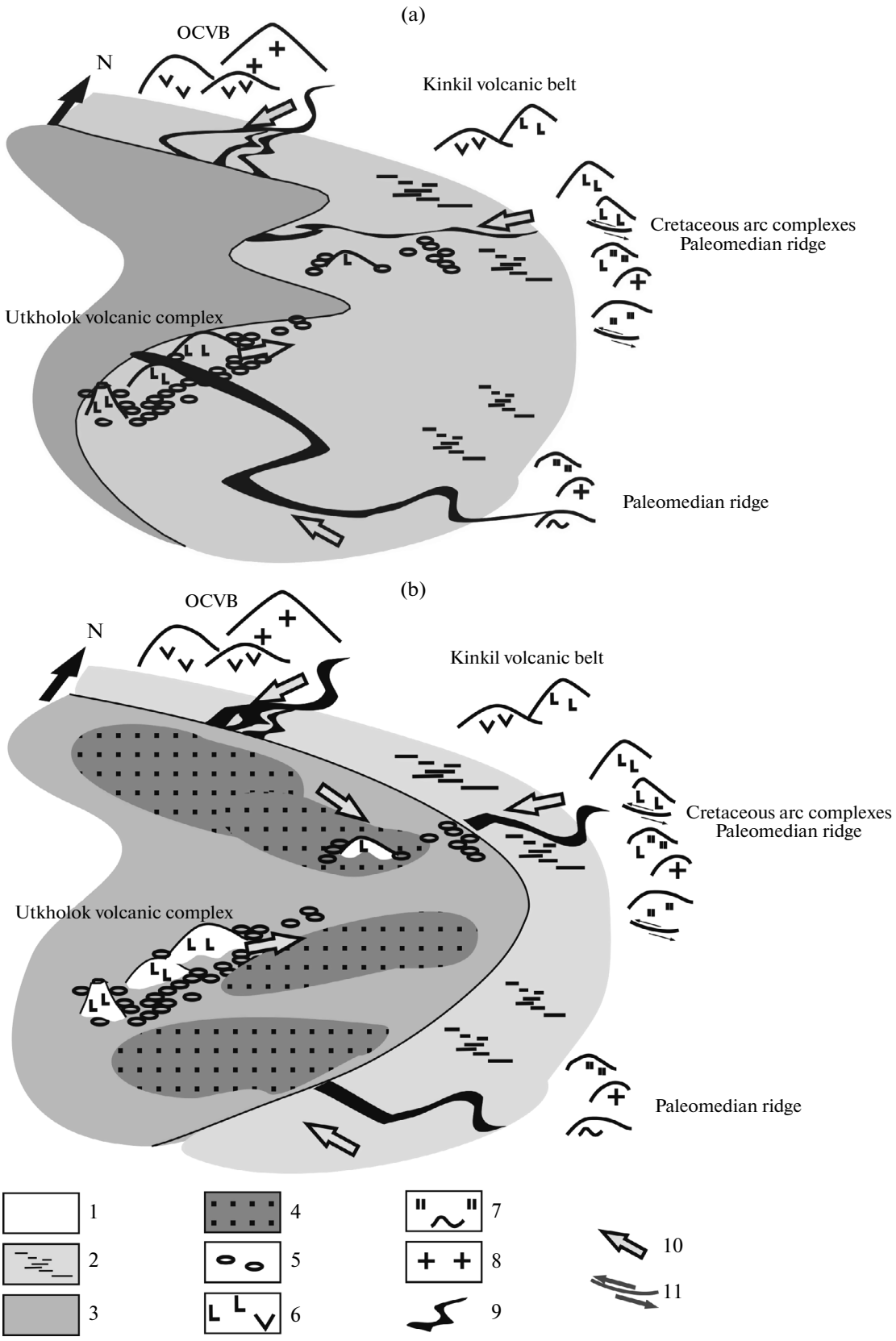

Fig. 12. Paleogeographic schemes of the central WKSB. (a) Early Eocene, (b) Middle Eocene. (1–3) Paleogeographic setting: (1) land, (2) land intermittently flooded by sea, (3) shallow sea; (4, 5) sediment type: (4) sandy silt, (5) conglomerates; (6–8) rock composition: (6) felsic, intermediate, and felsic volcanic rocks, (7) cherts and siliceous shales, (8) granitoids; (9) rivers; (10) direction of the clastic material transport; (11) overthrust.

25%) in the remaining samples (~250–110 Ma). The most significant peak is recorded in samples with the age of 106–77 Ma corresponding to calc-alkaline magmatism in the Okhotsk–Chukotka volcanic belt (Akinin et al., 2011) (Fig. 11). Younger zircon grains are rare in samples from the West Kamchatka trough (Fig. 11), probably, due to synchronous volcanism in the Kinkil volcanic belt. The Early Eocene peak is distinct only in sandstones of the Ukelayat flysch.

THE SNATOL (MIDDLE EOCENE) PALEOGEOGRAPHY OF WESTERN KAMCHATKA

To elucidate specific features of sedimentation in the Snatol time, two-member paleogeographic schemes were modeled for the early and late stages marked by deposition of the coarse-clastic sequence and psammitic material, respectively. During the early stage of the WKSB formation, sediments were accumulated in intermontane valleys and at foothills (Grigorenko, 1981, 2011). Sediments were deposited mainly in proluvial fans and mountain riverbeds. Composition and age of the pebble material of conglomerates suggest the existence of a proximal provenance. Basal conglomerates of WKSB are scrutinized in (Khisamutdinova et al., 2015). Clasts in conglomerates are dominated by volcanic rocks of the basic, intermediate, and less common felsic composition. Fragments of terrigenous rocks are subordinate. The K–Ar age of pebbles (51.5 ± 3.5, 51.2 ± 2.0, 35.5 ± 6.5, 87 ± 3.5, 50 ± 1.5, 57.3 ± 2 Ma) suggests the existence of two different-age (Late Cretaceous and Early Eocene) provenances. The clastic material was mainly derived from volcanic island-arc fragments, which were located east of the incipient basin (Solov'ev and Shapiro, 2011), and Paleogene volcanic complexes, which surrounded the basin from the east and occupied its central part (Fig. 12a).

Later, the coarse-clastic sequence was replaced by sandstones in response to marine transgression (Gladenkov et al., 1991, 1997). The basin began to accumulate fine-clastic material that was delivered from new sources located in the north and northeast, as suggested by measurements of oblique bedding. The main sources of clastic material in this time were represented by the Okhotsk–Chukotka volcanic belt located in the north-northwest, Achaivayam–Valagin island arc located in the east, and volcanic rocks of the Kinkil belt and Utkholok Peninsula. Some clastic material deposited in the southern parts of the basin could likely be derived from the Median Ridge of Kamchatka, which was exposed to erosion in the Middle Eocene (Fig. 12b).

CONCLUSIONS

Sandstones of the Middle Eocene Snatol Formation belong to the immature quartz–feldspar and feldspar–quartz graywackes, according to classification (Shutov, 1975). Clastic rock grains are mainly represented by the erosion products of volcanic rocks: fragments of volcanic glass and rocks with the felsitic, lathlike, and less common microclinic groundmass. The sandstone composition does not change much from the top to bottom of the sequence. It also remains constant along the lateral direction.

In diagram (Dickinson et al., 1983) characterizing the setting of provenances, most data points of these rocks fall into the mixed source domain, many points fall into the island-arc domain with different levels of the erosional section, and some points fall into the domain of disintegrating orogenic buildups. This conclusion is supported by the relationship between alkaline oxides and silica acidity of rocks, according to (Nesbitt and Young, 1982). Data points pertaining to this parameter make up a domain indicating a similar geodynamic setting of the eroded rock complexes.

The mineral composition of the heavy fraction of sandstones suggests the presence of two provenances with different compositions: (i) felsic igneous and volcanic rocks and (ii) mafic igneous rocks.

Morphology of clastic zircon crystals indicates the erosion of mainly subalkaline (calc-alkaline) granitoids and a subordinate share of high-alumina muscovite granites. This conclusion is consistent with the U–Pb isotope data on zircon from sandstones of the Snatol Formation. The sandstones were mainly derived from the Okhotsk–Chukotka volcanic belt that accommodates large volumes of the calc-alkaline igneous rocks, including the contaminated mantle–crust granitoids (Akinin et al., 2011).

ACKNOWLEDGMENTS

This work was supported by the Russian Foundation for Basic Research (project nos. 13-0500485_a, 12-05-31299 mol_a) and the Scientific School Program (project no. NSh 2981.2014.5).

REFERENCES

Akinin, V.V. and Miller, E.L., Evolution of calc-alkaline magmas of the Okhotsk–Chukotka volcanic belt, *Petrologiya*, 2011, vol. 19, no. 3, pp. 237–277.

Belonin, M.D., Grigorenko, Yu.N., Margulis, L.S., et al., *Razvedochnyi potentsial Zapadnoi Kamchatki i sopredel'nogo shel'fa (neft' i gaz)* (Exploration Potential of Western Kamchatka and Adjacent Shelf: Oil and Gas), St. Petersburg: Nedra, 2003.

Belousova, E.A., Griffin, W.L., and O'Reily, S.Y., Zircon crystal morphology, trace element signatures and Hf isotope composition as a tool for petrogenetic modelling: examples from Eastern Australian granitoids, *J. Petrol.*, 2006, vol. 47, no. 2, pp. 329–353.

Bogdanov, N.A. and Chekhovich, V.D., On the collision between the West Kamchatka and Sea of Okhotsk plates, *Geotectonics*, 2002, no. 1, pp. 63–75.

Bogdanov, N.A. and Dobretsov, N.L., The Okhotsk oceanic volcanic plateau, *Geol. Geofiz.*, 2002, vol. 43, no. 2, pp. 97–110.

Budantsev, L.Yu., Early Paleogene flora of western Kamchatka, in *Trudy GIN RAN* (Trans. GIN RAS), St. Petersburg: Nauka, 2006, no. 22.

Chase, F., *Kolichestvenno-mineralogicheskii analiz shlifov pod mikroskopom* (Quantitative Mineralogical Analysis of Thin Sections under Microscope), Moscow: IL, 1963.

Chekhovich, V.D., *Tektonika i geodinamika skladchatogo obramleniya malykh okeanicheskikh basseinov* (Tectonics and Geodynamics of the Folded Framing of Minor Oceanic Basins), Moscow: Nauka, 1993.

Dickinson, W.R., Beard, L.S., Brakenridge, G.R., et al., Provenance of North American Phanerozoic sandstones in relation to tectonic setting, *Geol. Soc. Am. Bull.*, 1983, vol. 94, pp. 222–235.

Dmitrieva, T.V., Applied aspects of micropaleontology: Evidence from foraminifers in Upper Paleogene and Neogene productive rocks of western Kamchatka, in *Neftegazovaya geologiya. Teoriya i praktika* (Petroleum Geology: Theory and Practice), 2007. http://www.ngtp.ru/rub/2/027.pdf

Gehrels, G.E., Detrital zircon U-Pb geochronology: Current methods and new opportunities, in *Recent Advances in Tectonics of Sedimentary Basins*, Busby, C. and Azor, A., Eds., Azor: Wiley-Blackwell, 2011, pp. 47–62.

Gehrels, G.E., Valencia, V.A., and Ruiz, J., Enhanced precision, accuracy, efficiency, and spatial resolution of U-Pb ages by laser ablation-multicollector-inductively coupled plasma-mass spectrometry, *Geochem., Geophys., Geosyst.*, 2008, vol. 9, p. Q03017. doi:10.1029/2007GC001805.

Gladenkov, Yu.B., Sinel'nikova, V.N., Shantser, A.E., et al., The Eocene of western Kamchatka, in *Trudy GIN RAN* (Trans. GIN RAS), Moscow: Nauka, 1991, no. 467.

Gladenkov, Yu.B., Shantser, A.E., Chelebaeva, A.I., et al., Lower Paleogene of western Kamchatka: Stratigraphy, paleogeography, and geological events, in *Trudy GIN RAN* (Trans. GIN RAS), Moscow: GEOS, 1997, no. 488.

Gladenkov, Yu.B., Shantser, A.E., Chelebaeva, A.I., and Sinel'nikova, V.N., Early Paleogene geological events in the western Kamchatka region, *Stratigr. Geol. Correlation*, 1998, vol. 6, no. 5, pp. 495–508.

Gladenkov, Yu.B., Sinel'nikova, V.N., Chelebaeva, A.I., and Shantser, A.E., *Biosfera – ekosistema – biota v proshlom Zemli. Ekosistemy kainozoya Severnoi Patsifiki. Eotsen - oligotsen Zapadnoi Kamchatki i sopredel'nykh raionov* (Biosphere, Ecosystem, and Biota in the Earth's Past: Cenozoic Ecosystem in the North Pacific, Eocene–Oligocene in Western Kamchatka and Adjacent Regions), Moscow: GEOS, 2005.

Grigorenko, Yu.N., The graywacke formation of western Kamchatka, in *Litologo-petrograficheskie issledovaniya v neftyanoi geologii* (Lithopetrographic Studies in Petroleum Geology), St. Petersburg: VNIGRI, 1969, no. 279, pp. 58–79.

Grigorenko, Yu.N., Types and associations of clastic rocks in Paleogene suites of western Kamchatka, in *Kainozoi Dal'nego Vostoka* (The Cenozoic of the Far East), St. Petersburg: VNIGRI, 1981, pp. 63–91.

Grigorenko, Yu.N., *Paleotsen-eotsenovyi grauvakkovyi kompleks tylovykh progibov Pritikhookeanskoi okrainy (stroenie i formirovanie)* (The Paleocene–Eocene Graywacke Complex in Rear-Arc Troughs of the Pacific Margin: Structure and Formation), St. Petersburg: VNIGRI, 2011.

Hourigan, J.K., Brandon, M.T., Soloviev, A.V., et al., Eocene arc-continent collision and crustal consolidation in Kamchatka, Russian Far East, *Am. J. Sci.*, 2009, vol. 309, pp. 333–396.

Karta poleznykh iskopaemykh Kamchatskoi oblasti. Masshtab 1 : 500000 (Map of Mineral Resources in the Kamchatka Region. Scale 1 : 500000), Litvinov, A.F, Patok, M.G, and Markovskii, B.A, Eds., St. Petersburg: VSEGEI, 1999.

Khanchuk, A.I., *Evolyutsiya drevnei sialicheskoi kory v ostrovoduzhnykh sistemakh vostochnoi Azii* (Evolution of the Ancient Sialic Crust in Island-Arc Systems of East Asia), Vladivostok: DVNTs AN SSSR, 1985.

Khisamutdinova, A.I., Zakharov, D.O., and Solov'ev, A.V., Provenances of basal conglomerates in the West Kamchatka sedimentary basin: Age and composition of pebbles, *Russ. J. Pac. Geol.*, 2016, no. 3, pp. 1–20.

Konstantinovskaia, E.A., Arc-continent collision and subduction reversal in the Cenozoic evolution of the Northwest Pacific: An example from Kamchatka (NE Russia), *Tectonophysics*, 2001, vol. 333, pp. 75–94.

Kopchenova, E.V., *Mineralogicheskii analiz shlikhov i rudnykh kontsentratov* (Mineralogical Analysis of Panned Fractions and Ore Concentrates), Moscow: Nedra, 1979.

Ludwig, K.R., User's manual for Isoplot 3.0: A geochronological toolkit for Microsoft Excel, *Berkeley Geochronology Center, Berkeley, California*, 2003, Spec. Publ. 4.

Malinovsky, A.I. and Markevich, P.V., Heavy clastic minerals from the Far East island-arc complexes, *Russ. J. Pac. Geol.*, 2007, vol. 26, no. 1, pp. 71–81.

Mange, M.A. and Otvos, E.G., Gulf coastal plain evolution in West Louisiana: Heavy mineral provenance and Pleistocene alluvial chronology, *Sedim. Geol.*, 2005, vol. 182, pp. 29–57.

Moiseev, A.V. and Solov'ev, A.V., New data on deformations of Tertiary rocks in western Kamchatka (Tigil region), *Geol. Razved.*, 2010, no. 1, pp. 13–19.

Morton, A.C., Heavy minerals in provenance studies, in *Provenance of Arenites*, Zuffa, G.G., Ed., Dordrecht: Reidel, 1985, pp. 249–277.

Morton, A.C. and Hallsworth, C.R., Identifying provenance-specific features of detrital heavy mineral assemblages in sandstones, *Sedim. Geol.*, 1994, vol. 90, pp. 241–256.

Morton A.C., Hallsworth C.R., Processes controlling the composition of heavy mineral assemblages in sandstones, *Sedim. Geol.*, 1999, vol. 124, pp. 3–29.

Morton, A.C., Whitham A.G., and Fanning, C.M., Provenance of Late Cretaceous to Paleocene submarine fan sandstones in the Norwegian Sea: Integration of heavy mineral, mineral chemical and zircon age data, *Sedim. Geol.*, 2005, vol. 182, pp. 3–28.

Nesbitt, H.W. and Young, G.M., Petrogenesis of sediments in the absence of chemical weathering, effects of abrasion and sorting on bulk composition and mineralogy, *Sedimentology*, 1982, vol. 43, pp. 341–358.

Nesbitt, H.W. and Young, G.M., Prediction of some weathering trends of plutonic and volcanic rocks based on ther-

modynamic and kinetic considerations, *Geochim. Cosmochim. Acta*, 1984, vol. 48, pp. 1523–1534.

Nokleberg, W.J., Parfenov, L.M., Monger, J.M.H., et al., Phanerozoic tectonic evolution of the circum-north Pacific, *US Geol. Surv. Open File*, 1998, Report 98-754.

Ob"yasnitel'naya zapiska k tektonicheskoi karte Okhotomorskogo regiona masshtaba 1 : 2 00000 (Explanatory Note to Tectonic Map of the Sea of Okhotsk Region, Scale 1 : 500000) Bogdanov, N.A. and Khain, V.E, Eds., Moscow: ILOVM RAN, 2000.

Otchet po teme "Obrabotka materialov bureniya parametricheskikh skvazhin Tigil'skogo raiona Zapadnoi Kamchatki" (Report on "Processing of Materials from Parametric Boreholes in the Tigil Region, Western Kamchatka"), Goma, L.V., Ed., Leningrad: RFGF, 1986.

Parfenov, L.M., Natapov, L.M., Sokolov, S.D., and Tsukanov, N.V., Terrains and accretionary tectonics of Northeast East, *Geotektonika*, 1993, no. 1, pp. 68–78.

Pupin, J.P., Zircon and granite petrology, *Contr. Miner. Petrol.*, 1980, vol. 73, pp. 207–220.

Resheniya rabochikh Mezhvedomstvennykh regional'nykh stratigraficheskikh soveshchanii po paleogenu i neogenu vostochnykh raionov Rossii – Kamchatki, Koryakskogo nagor'ya, Sakhalina i Kuril'skikh ostrovov (Resolutions of Working Interdepartmental Regional Stratigraphic Conferences Devoted to Paleogene and Neogene in Eastern Russia – Kamchatka, Koryak Highland, Sakhalin, and Kuril Islands), Moscow: GEOS, 1998, p. 146.

Rosen, O.M., Siberian craton - a fragment of a Paleoproterozoic supercontinent, *Russ. J. Earth Sci.*, 2002, vol. 4, pp. 103–119.

Roser, B.P. and Korsch, R.J., Determination of tectonic setting of sandstone-mudstone suites using SiO_2 content and K_2O/Na_2O ratio, *J. Geol.,* 1986, vol. 94, pp. 635–650.

Rozhkova, D.V., Solov'ev, A.V., Khisamutdinova, A.I., and Ipat'eva, I.S., Informativity of clastic zircon in reconstructions of provenances: Evidence from Paleogene of the West Kamchatka Basin, *Byull. MOIP. Otd. Geol.*, 2012, vol. 87, no. 6, pp. 57–62.

Safonova, I., Maruyama, S., Hirata, T., et al., LA-ICP-MS U-Pb ages of detrital zircons from Russia's largest rivers: Implications for major granitoid events in Eurasia and global episodes of supercontinent formation, *J. Geodyn.*, 2010, vol. 50, pp. 134–153.

Serova, M.Ya., *Foraminifery i biostratigrafiya verkhnego paleogena Severnoi Patsifiki* (Upper Paleogene Foraminifers and Biostratigraphy of the North Pacific, Moscow: Nauka, 2001.

Shutov, V.D., Mineral'nye paragenezisy grauvakkovykh kompleksov, in *Trudy GIN AN SSSR* (Trans. GIN AN), Moscow: Nauka, 1975.

Shvanov, V.N., *Petrografiya peschanykh porod (komponentnyi sostav, sistematika i opisanie mineral'nykh vidov)* (Petrography of Sandy Rocks: Component Composition, Systematics, and Description of Mineral Species), Leningrad: Nedra, 1987.

Skhema tektonicheskogo raionirovaniya. Dal'nevostochnyi federal'nyi okrug, Kamchatskii krai (Schematic Tectonic Regionalization. Far East Federal District. Kamchatka Territory), St. Petersburg: VSEGEI, 2001. http://vsegei.ru/ru/info/gisatlas/dvfo/kamchatka/tecton_rai.jpg

Sokolov, S.D., *Akkretsionnaya tektonika Koryaksko-Chukotskogo segmenta Tikhookeanskogo poyasa* (Accretionary Tectonics of the Koryak–Chukotka Segment of the Pacific Belt), Moscow: Nauka, 1992.

Solov'ev, A.V., Tectonics of western Kamchatka based on the Track Dating and structural analysis, in *Zapadnaya Kamchatka: geologicheskoe razvitie v mezozoe* (Western Kamchatka: Geological Evolution in the Mesozoic), Moscow: Nauchn. Mir, 2005, pp. 163–194.

Solov'ev, A.V., *Izuchenie tektonicheskikh protsessov v oblastyakh konvergentsii litosfernykh plit: metody trekovogo datirovaniya i strukturnogo analiza* (Study of Tectonic Processes in Convergence Zones of Lithospheric Plates: Methods of the Track Dating and Structural Analysis), Moscow: Nauka, 2008.

Solov'ev, A.V. and Shapiro, M.N., Eocene geodynamics of the northeastern margin of Asia(eastern Koryak region, Kamchatka, in *Geologicheskie protsessy v obstanovkakh subduktsii, kollizii i skol'zheniya litosfernykh plit* (Geological Processes during Subduction, Collision, and Sliding of Lithospheric Plates), Vladivostok, 2011, pp. 132–134.

Stavsky, A.P., Chekhovich, V.D., Kononov, M.V., and Zonenshain, L.P., Plate tectonics and palinspastic reconstruction of the Anadyr–Koryak region, Northeast USSR, *Tectonics*, 1990, vol. 9, pp. 81–101.

Til'man, S.M. and Bogdanov, N.A., *Tektonicheskaya karta Severo-Vostoka Azii. Ob"yasnitel'naya zapiska* (Tectonic Map of Northeast Asia: Explanatory Note), Moscow: Inst. Litosf., 1992.

Watson, B.F. and Fujita, K., Tectonic evolution of Kamchatka and the Sea of Okhotsk implications for the Pacific Basin, in *Tectonostratigraphic terranes of the Circum-Pacific region*, Howell, D.G., Ed., Houston: *Circ. Pac. Counc. Energy Miner. Resour.,* 1985, pp. 333–348.

Worrall, D.M., Tectonic history of the Bering Sea and the evolution of the Tertiary strike-slip basins of the Bering shelf, *Geol. Soc. Am.,* 1991, Spec. Pap. 257.

Zinkevich, V.P., Konstantinovskaya, E.A., Tsukanov, N.V., et al., *Akkretsionnaya tektonika Vostochnoi Kamchatki* (Accretionary Tectonics of Eastern Kamchatka), Moscow: Nauka, 1993.

Zonenshain, L.P., Kuz'min, M.I., and Natapov, L.M., *Tektonika litosfernykh plit territorii SSSR* (Tectonics of Lithospheric Plates in the Soviet Union), Moscow: Nauka, 1990, vol. 2.

Translated by D. Sakya